doi:10.1016/j.jmb.2011.04.018 J. Mol. Biol. (2011) 409, 722–741

Contents lists available at www.sciencedirect.com

Journal of Molecular Biology

journal homepage: http://ees.elsevier.com.jmb

Structural Features and Chaperone Activity of the NudC Protein Family

Meiying Zheng[1], Tomasz Cierpicki[1], Alexander J. Burdette[2,3], Darkhan Utepbergenov[1], Paweł Ł. Janczyk[1,4], Urszula Derewenda[1], P. Todd Stukenberg[4], Kim A. Caldwell[2,3] and Zygmunt S. Derewenda[1]*

[1]*Department of Molecular Physiology and Biological Physics, University of Virginia School of Medicine, Charlottesville, VA 22908, USA*
[2]*Department of Biological Sciences, University of Alabama, Tuscaloosa, AL 35487, USA*
[3]*Department of Neurobiology, Neurology, Center for Neurodegeneration and Experimental Therapeutics, University of Alabama at Birmingham, Birmingham, AL 35294, USA*
[4]*Department of Biochemistry and Molecular Genetics, University of Virginia School of Medicine, Charlottesville, VA 22908, USA*

Received 17 February 2011; received in revised form 7 April 2011; accepted 7 April 2011
Available online 21 April 2011

Edited by I. Wilson

Keywords:
protein structure;
crystallography;
nuclear migration;
chaperones;
protein–protein interactions

The NudC family consists of four conserved proteins with representatives in all eukaryotes. The archetypal *nudC* gene from *Aspergillus nidulans* is a member of the *nud* gene family that is involved in the maintenance of nuclear migration. This family also includes *nudF*, whose human orthologue, Lis1, codes for a protein essential for brain cortex development. Three paralogues of NudC are known in vertebrates: NudC, NudC-like (NudCL), and NudC-like 2 (NudCL2). The fourth distantly related member of the family, CML66, contains a NudC-like domain. The three principal NudC proteins have no catalytic activity but appear to play as yet poorly defined roles in proliferating and dividing cells. We present crystallographic and NMR studies of the human NudC protein and discuss the results in the context of structures recently deposited by structural genomics centers (i.e., NudCL and mouse NudCL2). All proteins share the same core CS domain characteristic of proteins acting either as cochaperones of Hsp90 or as independent small heat shock proteins. However, while NudC and NudCL dimerize *via* an N-terminally located coiled coil, the smaller NudCL2 lacks this motif and instead dimerizes as a result of unique domain swapping. We show that NudC and NudCL, but not NudCL2, inhibit the aggregation of several target proteins, consistent with an Hsp90-independent heat shock protein function. Importantly, and in contrast to several previous reports, none of the three proteins is able to form binary complexes with Lis1. The availability of structural information will be of help in further studies on the cellular functions of the NudC family.

*Corresponding author. E-mail address: zsd4n@virginia.edu.

Present addresses: M. Zheng, Monsanto Company, 800 North Lindbergh Boulevard, St. Louis, MO 63167, USA; T. Cierpicki, Department of Pathology, University of Michigan, Ann Arbor, MI 48109, USA.

Abbreviations used: NudCL, NudC-like; NudCL2, NudC-like 2; PDB, Protein Data Bank; HSQC, heteronuclear single-quantum coherence; SeMet, selenomethionine; CS, CHORD-Sgt1; NOE, nuclear Overhauser enhancement; MDH, malate dehydrogenase; ITC, isothermal titration calorimetry; GST, glutathione *S*-transferase; MBP, maltose binding protein; TEV, tobacco etch virus.

Introduction

The *nud* (*nu*clear *d*istribution) gene family was originally identified in the filamentous fungus *Aspergillus nidulans* (or *Emericella nidulans* in its sexual form) as a set of genes associated with dynein-dependent nuclear migration.[1–6] In a healthy organism, the nuclei migrate towards the growing tip of hyphae during vegetative growth,[5] whereas in mutants with impaired *nud* genes, the nuclei are clustered together following karyokinesis and are unable to undergo translocation.[2] The *nud* family became a focus of intense interest when it was discovered that one of its members, *nudF*, encoded a close homologue (42% amino acid sequence identity) of the mammalian Lis1 protein, which is mutated in a debilitating developmental genetic syndrome known as Miller–Dieker lissencephaly.[3,7–9] In afflicted individuals, the brain cortex is smooth (without typical groves or sulci) because the layer structure is partly or wholly disrupted due to the inability of young neurons to migrate from the ventricular zone to their target destinations. Thus, there has been considerable speculation that the nuclear migration pathway observed in *Aspergillus* has been evolutionarily conserved and acquired a new function in fetal brain development.

As expected, some of the *nud* genes code for the components of cytoplasmic motor dynein and dynactin, which are directly responsible for the translocation of the nucleus along microtubules.[10] Three *nud* genes do not belong to this group: *nudF*, *nudE*, and *nudC*. As already stated, the 45-kDa NudF is a homologue of the mammalian Lis1 protein, which is now known to be a dynein regulator and a component of the brain isoform of the platelet-activating factor acetylhydrolase II.[11,12] The NudE protein is represented in mammalian genomes by two paralogues, NudE and NudEL, currently renamed Nde1 and Ndel1.[13–15] Each protein, just over 300 residues in length, contains a conserved 160-residue-long parallel coiled-coil domain at the N-terminus, which binds the homodimeric Lis1.[16] The details of how this complex interacts with and regulates dynein are still being debated on, but recent data suggest that Lis1 alone, or with Nde1/Ndel1, induces a persistent force state in dynein.[17]

Of all the *nud* gene products, NudC has been the most elusive with respect to function. Deletion of the *nudC* gene in *Aspergillus* produces a severe phenotype with a much thicker cell wall compared to wild type.[18] Recently published data suggest that NudC and NudF form a complex in the fungus that is essential for the proper functioning of spindle pole bodies.[19] Orthologues of NudC have been identified in higher eukaryotes, including *Caenorhabditis elegans*,[20] *Drosophila melanogaster*,[21] amphibians (newt),[22] and mammals. In most—if not all—Metazoa, three paralogues are found: hNudC,[23,24] hNudC-like (NudCL, also annotated as NudC domain containing protein 3),[25] and hNudC-like 2 (NudCL2, or NudC domain containing protein 2).[26] The lengths of polypeptide chains differ among the three, but they all contain a single globular domain with significant amino acid sequence conservation.[27] A similar domain is also found in the fourth member of this family, NudCD1 (NudC domain containing protein 1).[28,29] This enigmatic protein (also known as CML66) is a tumor antigen that has been implicated in stimulating tumor cell proliferation, invasion, and metastasis, but its function is unknown.[28]

The physiological functions of the mammalian NudC paralogues are far from understood. The vast majority of the reported research focused on NudC. It is expressed in all tissues, both in the fetus and in the adult organism,[24] but at a particularly high level in the cell lines and proliferating cells of normal tissues,[30] indicating a possible role in cell division. Indeed, downregulation of human NudC mRNA results in impairment of both cell proliferation and mitotic spindle formation.[31] There is also evidence that NudC is involved in cytokinesis in a phosphorylation-dependent fashion.[32–34] As might be expected, a protein involved in mitotic cell division is also found to play a role in cancer. For example, there is an inverse correlation between NudC expression and nodal metastasis in esophageal cancer,[35] and an adenovirus expressing NudC was able to inhibit the growth of prostate tumors by blocking cell division.[36] In apparent contrast, NudC was identified as one of the overexpressed genes in cutaneous T-cell lymphoma[37] and was found to be expressed in neuroectodermal tumors, but not in nonneoplastic brain tissues.[38] Moreover, high expression levels were associated with cells infiltrating white matter or undergoing division.[38]

Unfortunately, the details of the specific molecular mechanisms in which NudC is involved are very elusive. Several reports implicate NudC in direct interactions with Lis1;[39–42] others suggest interactions with kinesin-1[43] and polo-like kinase.[32,44] A recent study lists 131 (sic) proteins identified by mass spectrometry as potential binding partners of NudC.[40] Furthermore, there is evidence that NudC may function as a chaperone, effectively stabilizing its target proteins or enhancing folding. This potentially includes both the Hsp90-dependent pathway[40] and direct chaperone activity.[40,44] Finally, there is a set of studies exploring the hypothesis that NudC is a secreted protein that functions by binding to the extracellular domain of the thrombopoietin receptor.[45–50]

The remaining two paralogues, NudCL and NudCL2, were discovered only recently and are just beginning to attract attention. So far, NudCL has been implicated in enhancing the stability of the dynein intermediate chain,[25] while NudCL2 has

been implicated in stabilizing Lis1 through the Hsp90 pathway.[26] An exhaustive review of *nudC*-like genes has appeared recently.[51]

To better understand structure–function relationships in the NudC family, we undertook a systematic structural characterization of hNudC using heteronuclear NMR and X-ray crystallography. While this work was in progress, several structures of NudC homologues, or their fragments, were deposited in the Protein Data Bank (PDB) by structural genomics centers. In this article, we take advantage of this novel information and present an overview of the structural features of the NudC family. Furthermore, we revisit the question on the interactions of NudC proteins with Lis1 and their intrinsic chaperone activities.

Results and Discussion

The amino acid sequence features of NudC family proteins: An overview

A number of important features relevant to the molecular architecture of the NudC protein family can be inferred from amino acid sequence comparisons (Fig. 1; Supplementary Fig. 1).

The prototypical member of the NudC family, the *A. nidulans* protein, contains 198 amino acids. The first 30 amino acids show a propensity to form coiled coil, as inferred from sequence-based prediction.[52] It has been predicted that a single globular domain, with apparent similarity to p23 and other small heat shock proteins,[27] spans residues 36–116. Downstream of this domain, secondary structure prediction strongly suggests the presence of two α-helices: one spanning residues 147–164 and one spanning residues 171–185. This architecture is conserved among known homologues from other filamentous fungi, including *Neosartorya*, *Penicillium*, *Ajellomyces*, and so on. The *nudC* gene is stringently conserved in all of Eukaryota, including protozoans (*Trypanosoma*, *Chlorella*, *Chlamydomonas*, etc.), invertebrates (*C. elegans*, *Drosophila*, *Anopheles*, etc.), plants (*Populus*, *Ricinus*, *Zea*, *Arabidopsis*, etc.), and vertebrates (zebra fish, salmon, newt, African clawed frog, chicken, dog, mouse, human, etc.). The only significant difference is that the N-terminal portion in higher eukaryotes is longer than that in fungi. In plants (e.g., *Zea mays*), it is ~135 residues long, with pronounced propensity for a coiled coil within the 60–130 fragment. Among metazoans, it is 150–160 residues in length, and the predicted coiled-coil element (residues 60–135) is separated from the globular domain by a 20-residue linker. Interestingly, the most conserved elements are outside the globular domain; in vertebrates, a stretch from residue 10 through reside 43 (human NudC numbering) is nearly fully conserved between a range of species, as is the C-terminal fragment downstream of the p23-like domain.

A homologous gene coding for the NudCL protein has so far been identified only in the animal

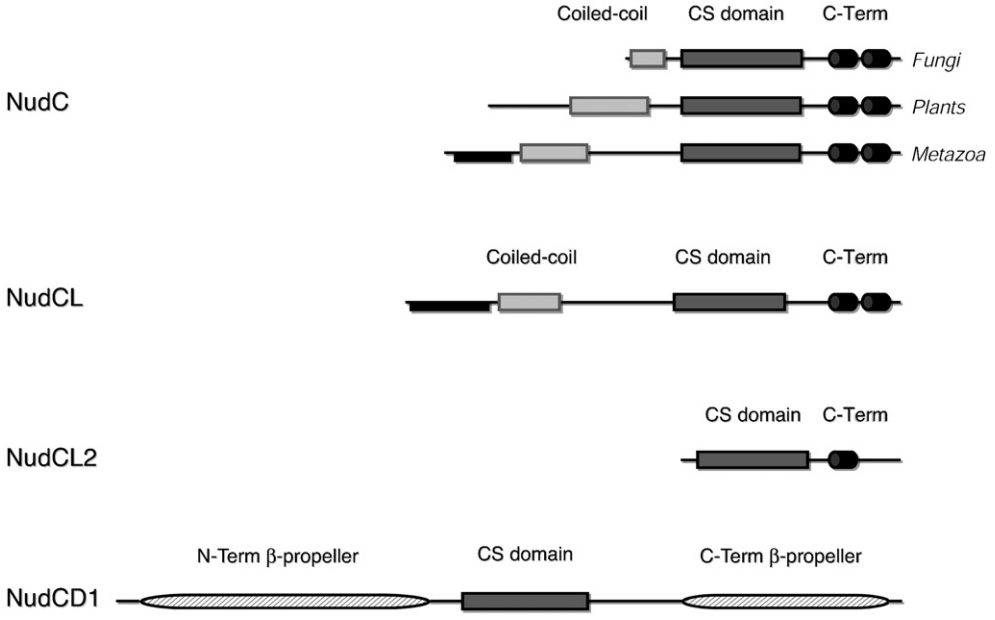

Fig. 1. The molecular architecture of proteins in the NudC family. The CS domain is shown in dark gray. The C-terminal black α-helices and the black intrinsically disordered fragment at the N-terminus are regions of the highest amino acid conservation within the NudC and NudCL subfamilies. The two putative β-propeller sections (hashed) shown for NudCD1 are likely to constitute two halves of a split domain.

kingdom and appears as low on the evolutionary ladder as *Platyhelminthes* (flatworms), but is then found all the way up to humans. The sequence features of the NudCL protein, which is typically slightly longer than NudC, are very similar, except that the putative coiled coil spans fewer residues (residues 75–99). There is also strong conservation in the NudCL subfamily; in vertebrates, there are three nearly completely conserved fragments: one at the N-terminus (residues 10–58) and two within the predicted α-helices at the C-terminus. However, these fragments differ significantly between the NudC subfamily and the NudCL subfamily: there is only ~30% amino acid identity within the N-terminal fragment between human NudC and NudCL, and ~25% identity between the C-terminal α-helices in the two proteins.

The third of the *nudC* family of genes, the NudCL2-coding gene, appears to be ubiquitous in all eukaryotes. It is different from both NudC and NudCL in that it lacks the entire N-terminal extension, while the C-terminal fragment downstream of the putative p23-like domain, about 50 residues in length, contains a single predicted α-helix (residues 110–130 in the human sequence). There is only limited amino acid similarity between the globular domain of NudCL2 and either NudC or NudCL, with 15–20% amino acid identity; the C-terminal portion, including the predicted helix, which is stringently conserved with the NudCL2 subfamily, bears no resemblance to the corresponding fragments in either NudC or NudCL.

The fourth distant relative is NudCD1, which appears to be a product of gene shuffling. The protein is found throughout Metazoa, including *Trichoplax adhaerens*, the sole member of the phylum Placozoa and the simplest known metazoan with only 11,514 protein coding genes.[53] Among vertebrates, it is highly conserved and occurs as two splicing variants 583 and 554 amino acids in length. Aside from the NudC-like domain in the center of the polypeptide chain, the remainder of the sequence does not resemble any known protein family. However, we used 3D-Jury[54,55] to predict the tertiary folds of the N-terminal and C-terminal regions, and we obtained results strongly suggesting that both regions contain partial β-propeller folds. Based on these results, it seems possible that the NudC-like domain has been inserted into a split canonical seven-blade β-propeller. The functional consequences of this unusual architecture cannot be predicted. Because this protein is only distantly related to the three principal paralogues, it was not a subject of our experimental investigation.

Identifying the boundaries of folded globular domain in hNudC

Although sequence analysis suggested that the globular domain in hNudC is limited to ~80 amino acids, a high level of sequence conservation extending into the C-terminus prompted us to investigate the actual structural boundaries of the globular domain using heteronuclear NMR spectroscopy. Samples of ^{15}N-labeled variants of different lengths were prepared, and heteronuclear single-quantum coherence (HSQC) spectra were recorded (Fig. 2). The fragment encompassing residues 143–331

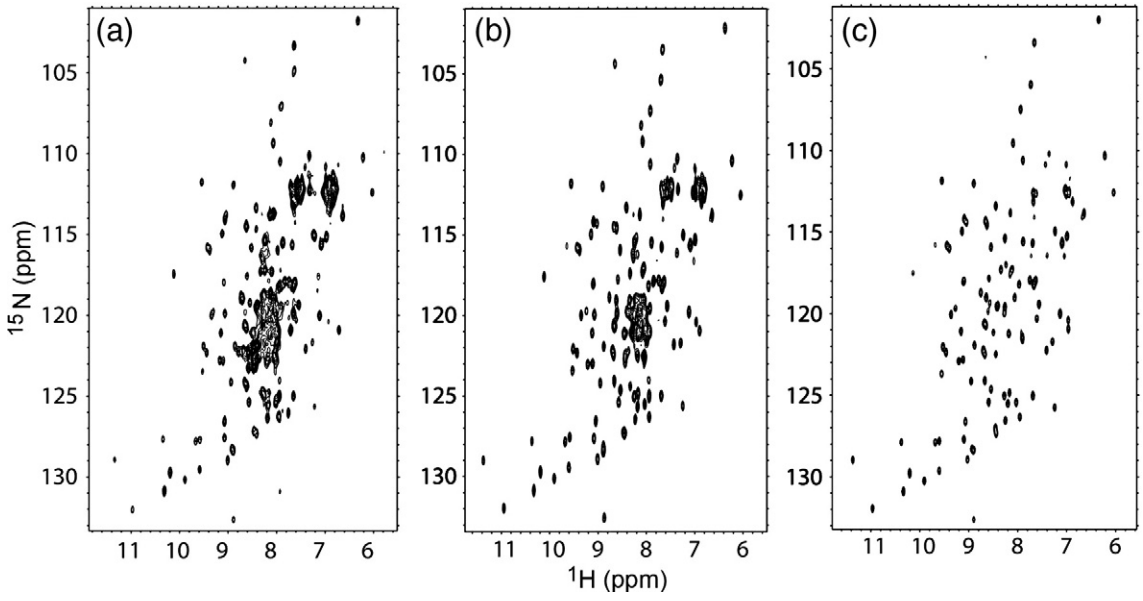

Fig. 2. NMR two-dimensional HSQC spectra recorded for three different variants of hNudC: (a) hNudC$^{143–331}$, (b) hNudC$^{158–331}$, and (c) hNudC$^{158–274}$.

showed a significant number of poorly dispersed resonances, suggesting lack of secondary structure in a significant portion of the protein. Screening of variants with truncations at both ends ultimately yielded one variant encompassing residues 158–274, which showed a very well-dispersed spectrum, with no indication of disorder. Further truncations (e.g., residues 162–274) were accompanied by chemical shift changes in the core resonances, suggesting structural rearrangements (data not shown), and were not pursued any further.

The crystal structure of the CS domain of hNudC

The wild-type recombinant 158–274 fragment did not yield single crystals suitable for X-ray diffraction experiments. Therefore, we decided to apply the surface entropy reduction protocol[56–59] to obtain variants with enhanced crystallizability. Of the five variants tested, a double mutant, E236A,K239A, yielded good-quality crystals, and the structure was solved by multiwavelength anomalous diffraction phasing using selenomethionine (SeMet)-labeled protein. The atomic model was refined using data extending to 1.75 Å resolution. Crystallographic details are shown in Table 1.

The asymmetric unit of the crystal contains five independent copies of the molecule. In each case, there is interpretable electron density for all but the last one to two residues. The core of the molecule is formed by an all-antiparallel β-sandwich, with the larger sheet made up of strands 1, 2, 3, 8, and 7, and with the opposite smaller sheet made up of strands 4, 5, and 6. These strands are the only well-defined secondary structure elements within the domain, with ~60% of the residues occurring in loops, a 10-residue-long N-terminal extension, and a 29-residue-long C-terminal fragment (Fig. 3a). All five copies superpose very well (with pairwise r.m.s. differences of 0.1–0.3 Å between C^{α} positions), indicating that this tertiary fold is not influenced by crystal-packing forces and faithfully represents the structure of the protein in solution.

In general terms, the core of the molecule shares the tertiary fold with the Hsp90 cochaperone p23,[60] the Hsp20 chaperone, and α-crystallin core domains,[61] although there are differences in the loop structures, as well as in the exact numbers and lengths of the β-strands (Fig. 3c–e). As indicated by Dali,[62,63] the crystal structure of the hNudC core domain is most similar to the CHORD-Sgt1 (CS) domain of the *Arabidopsis thaliana* Sgt1a protein (Z score = 11.4; r.m.s.d. = 1.7 Å) even though amino acid sequence identity is only 13% (Fig. 3b). The Sgt1 protein, which is found in fungi, plants, and animals, is a cochaperone of Hsp90 and appears to play an important role in innate immunity.[64,65] Its 90-residue-long CS domain is smaller than the core hNudC domain in that it lacks the N-terminal fragment, including the first β-strand, while its C-terminal fragment is shorter.

There are also distinct similarities to the core domains of Sba1 (another Hsp90 cochaperone)[66] and Shq1p (an essential H/ACA ribonucleoparticle assembly protein whose function is unclear), although it is known to be independent of Hsp90.[67]

While the Pfam database[68,69] classifies the Hsp20/α-crystallin proteins separately (Hsp20 or PF00011), all other sequences are grouped together as the CS (PF04969) family, which currently contains over 1150 sequences. Among them is the functionally

Table 1. Crystallographic data

	SeMet peak	Refinement
Data collection		
Wavelength	0.97928	0.97928
Space group	$P2_1$	$P2_1$
Unit cell parameters		
a, *b*, *c* (Å)	66.73, 51.82, 92.85	66.73, 51.82, 92.85
β (°)	90.58	90.58
Resolution (Å)[a]	1.75 (1.81–1.75)	1.75 (1.81–1.75)
Number of total reflections	258,269	259,696
Number of unique reflections	124,203	63,806[b]
Redundancy	2.1 (1.9)	4.1 (3.7)
Completeness (%)	99.6 (97.4)	99.9 (99.0)
R_{sym} (%)[c]	7.1 (38.0)	9.9 (41.2)
$I/\sigma(I)$	11.9 (2.2)	12.0 (3.1)
Refinement statistics		
Model composition		5753 atoms (590 residues + 877 waters + 1 acetate ion)
Resolution limits (Å)		28–1.75
Reflections in working set/test set		60,523/3227
R_{cryst}[d]/R_{free} (%)		17.3/20.2
r.m.s.d. bond (Å)/angle (°)		0.006/1.03
Ramachandran plot		
Most favored regions (%)		457/90.7
Additionally allowed regions (%)		47/9.3
Generously allowed regions (%)		0/0.0
Disallowed regions (%)		0/0.0
Average atomic *B* values protein/water (Å^2)		26.1/34.2

[a] The numbers in parentheses describe the relevant value for the last resolution shell.

[b] ±Reflections from the SeMet peak data set were scaled together for the data set used in refinement.

[c] $R_{sym} = \sum |I_i - \langle I \rangle| / \sum I$, where I_i is the intensity of the ith observation, and $\langle I \rangle$ is the mean intensity of the reflections.

[d] $R_{cryst} = \sum ||F_{obs}| - |F_{calc}|| / \sum |F_{obs}|$, crystallographic R-factor, and $R_{free} = \sum ||F_{obs}| - |F_{calc}|| / \sum |F_{obs}|$, where all reflections belong to a test set of randomly selected data.

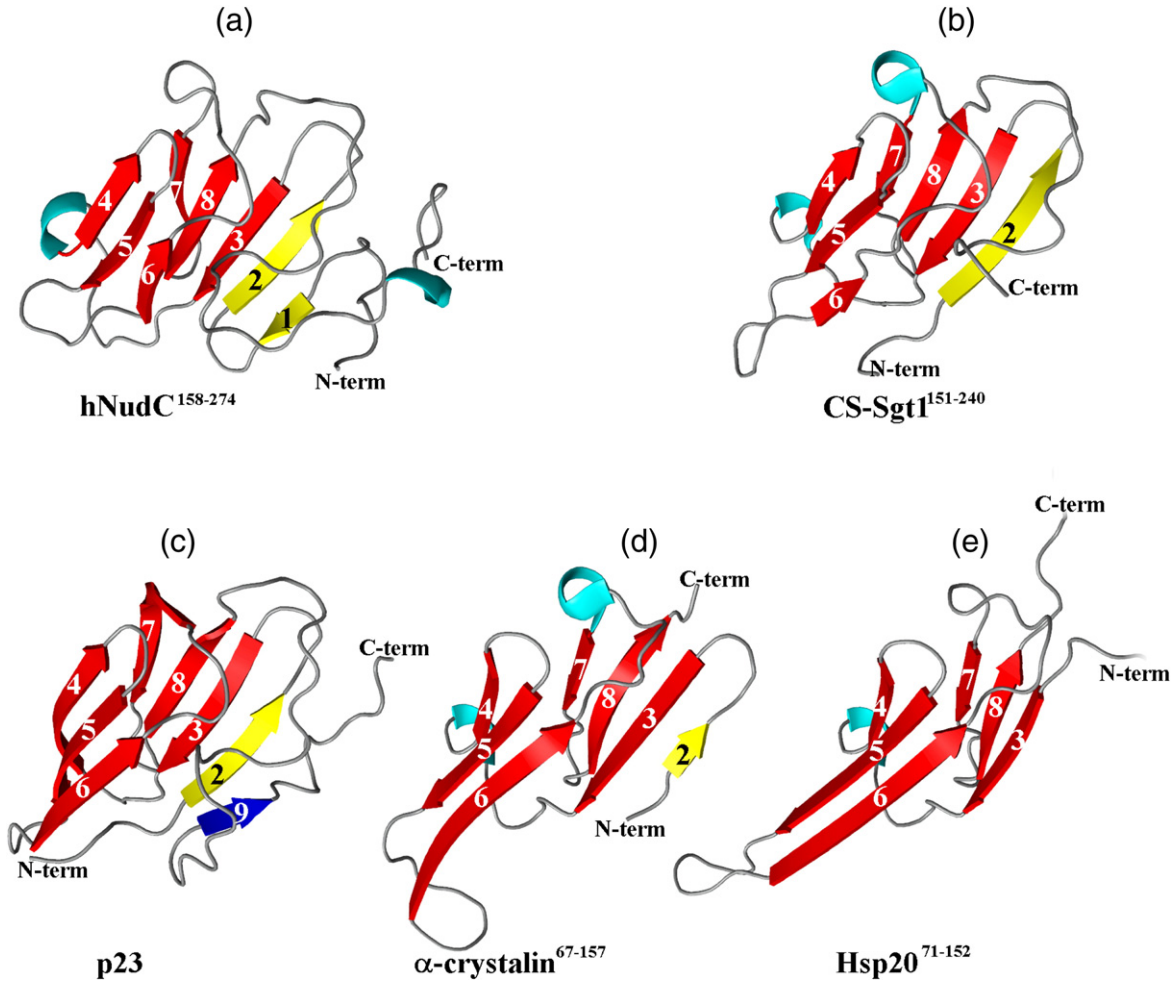

Fig. 3. A comparison of the crystal structure of the CS domain from hNudC residues 158–274 (a; this work; PDB ID: 3QOR) with those of (b) Sgt1 (PDB ID: 2XCM), (c) p23 (PDB ID: 1EJF), (d) α-crystallin (PDB ID: 2WJ7), and (e) rat Hsp20 (PDB ID: 2WJ5).

studied—but not structurally characterized—CS domain of the Siah1-interacting protein.[70,71] We will refer henceforth to the core domains of all NudC proteins as CS domains.

The conserved C-terminal fragment of hNudC

Our initial NMR experiments strongly suggested that the C-terminal fragment of hNudC (i.e., downstream of residue 274) is not a part of the CS domain, even though it shows stringent amino acid sequence conservation within the entire NudC subfamily. This is unexpected because, typically, such sequence conservation occurs within folded domains. Therefore, we decided to explore in more depth the question on the intrinsic structure of the C-terminus. In order to identify resonances corresponding to residues within the C-terminal fragment, we compared the HSQC spectra for $hNudC^{158–331}$ and $hNudC^{158–274}$ (Fig. 2b and c) and found 47 additional peaks for the longer construct, but with poor chemical shift dispersion. To ascertain whether the C-terminal fragment has any defined tertiary structure in solution, we measured $^{15}N\{^{1}H\}$ heteronuclear nuclear Overhauser enhancements (NOEs) for $NudC^{158–331}$. Interestingly, the vast majority of residues in the C-terminal region show positive heteronuclear NOEs with an average value of 0.70 ± 0.16, which strongly indicates that this fragment adopts some ordered structure. The very limited chemical shift dispersion observed in the HSQC spectra is consistent with the presence of an α-helical structure, in agreement with secondary structure prediction. We then asked if the C-terminal fragment interacts with the CS domain. A comparison of the HSQC spectra for $hNudC^{158–331}$ and $hNudC^{158–274}$ revealed that truncation of the C-terminus results in marginally small differences for the resonances within the CS domain. This strongly indicates that there are no significant contacts between the C-terminal α-helical fragment and the CS

domain; therefore, the C-terminal α-helix is free to tumble independently in solution.

The structure of CS domains in other NudC family proteins

While this work was in progress, a search of the PDB revealed several coordinate sets deposited for NudC family proteins by structural genomics centers.

The crystal structure of the protozoan *E. cuniculi* NudC homologue (PDB ID: 2O30) represents the shortest known NudC protein, essentially containing only the CS domain. A BLAST search shows that the sequence of this protein is most similar to plant homologues of NudC (39% amino acid identity to *Z. mays*), while it is most similar to hNudCL (29% identity) among human proteins. The CS domain of *E. cuniculi* NudC lacks the N-terminal first strand, and the loop structure makes it more similar to p23 (Fig. 4a).

There is no known crystal structure of the CS domain from NudCL, but there are two solution (NMR) structures (PDB IDs: 1WGV and 2CR0) of the fragments of the human and mouse proteins, respectively, which reveal a tertiary fold that is virtually identical, within experimental limits, to that seen in our crystal structure of the CS domain of hNudC (Fig. 4b).

The crystal structure of the full-length mouse NudCL2 (mNudCL2; PDB ID: 2RH0) shows several unexpected features. The core of the CS domain appears deceptively similar to that of hNudC, except that, downstream of the β8 strand (the last

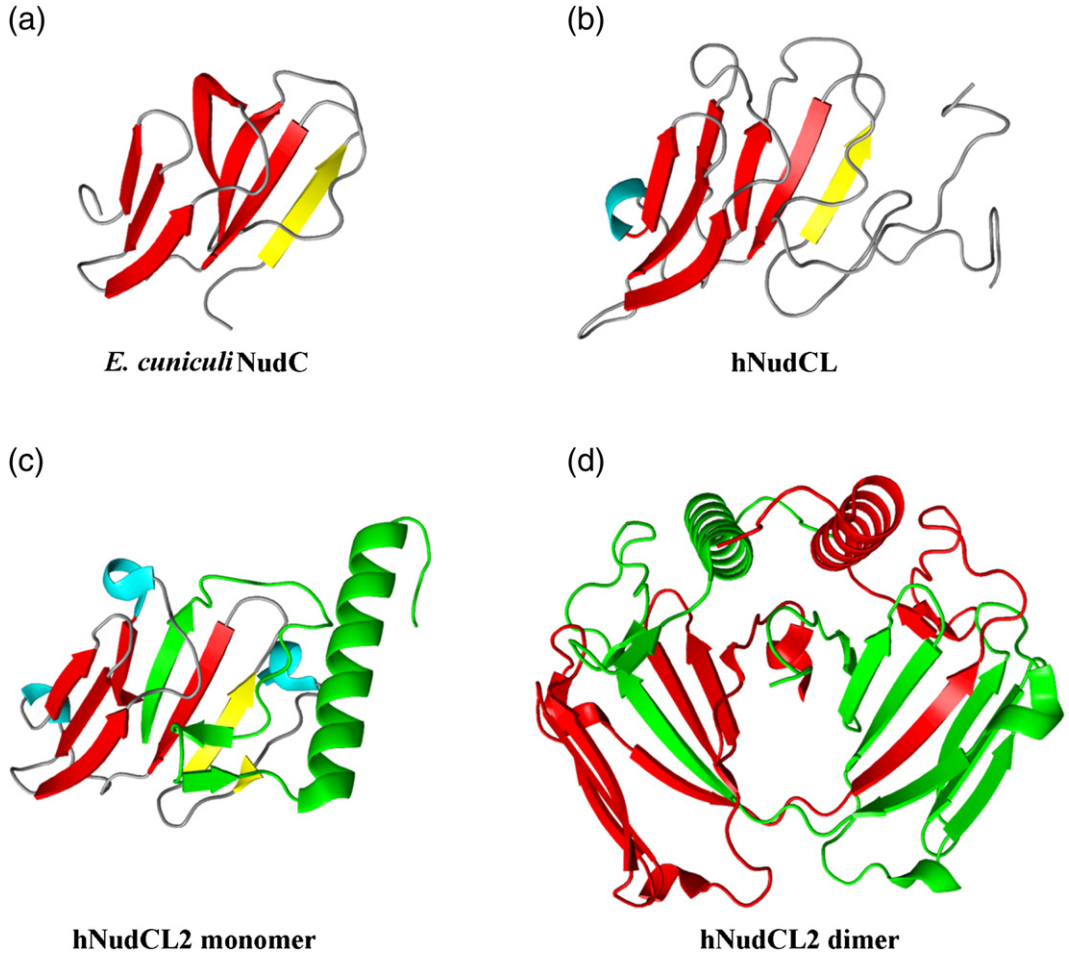

Fig. 4. The structures of CS domains from various NudC family proteins. In all figures, the core β-strands are shown in red, and the N-terminal strand is shown in yellow. (a) The crystal structure of the CS domain from *E. cuniculi* (PDB ID: 2O30; this structure was determined at 1.7 Å and refined to R/R_{free} of 0.217/0.256). (b) NMR structure (best of 20 conformers) of the 176–286 fragment of the CS domain from human NudCL (PDB ID: 1WGV). (c) The crystal structure of the full-length mouse NudCL2 (PDB ID: 2RH0; resolution, 1.95 Å; R/R_{free}, 0.192/0.235); only one 'monomer' is shown. The red and green fragments originate from two different molecules in the asymmetric unit. (d) Complete domain-swapped homodimer of NudCL2. The two molecules are depicted in red and green, respectively.

strand in the β-sandwich), there is a short antiparallel β-hairpin and a six-turn α-helix (Fig. 4c). Thus, unlike in NudC, the C-terminal fragment is a part of the globular entity. On closer inspection, the β8 strand and the downstream secondary structure elements originate from the neighboring monomer, creating a domain-swapped homodimer (Fig. 4d). The two C-terminal α-helices, one from each monomer, are aligned in this dimer in an antiparallel fashion and form a part of an intimate dimer interface.

An intriguing aspect of the mNudCL2 crystal structure is the assembly of the dimers into a filament by virtue of a noncrystallographic 2-fold screw axis, which is parallel with the crystallographic *a*-axis (Fig. 5). This filament is formed exclusively by the exposed faces of the two antiparallel α-helices (unique to NudCL2), which at each end contain a cluster of solvent-exposed hydrophobic residues: Trp113, Phe127, Phe134, and Phe136 (nearly 1100 $Å^2$ per dimer). The clusters from one dimer interlock with the dimers shifted in each direction by half of a molecule's length. The interface-forming exposed hydrophobic residues in the C-terminal helix are among the most conserved amino acids in the known NudCL2 amino acid sequences. This strongly suggests that the surface patch mediating this crystal contact may be biologically relevant and may be involved in hitherto unidentified protein–protein interactions.

Oligomeric state of NudC family proteins

Although the crystal structure of the hNudC CS domain contains five copies in the asymmetric unit, there is no indication that these molecules form specific oligomeric structures in solution, as is the case, for example, for Hsp20/α-crystallin proteins.[72] Moreover, the CS domain of hNudC and the $hNudC^{158–331}$ variant, which includes the C-terminal α-helix, are both distinctly monomeric in solution, as determined by gel filtration and as judged by NMR line widths (data not shown). In contrast, full-length hNudC migrates on gel filtration with an apparent molecular mass of ~140 kDa (data not shown), suggesting that it forms an oligomer. In view of the putative coiled coil within the N-terminal fragment of the mammalian NudC sequences, we wondered if this motif was responsible for protein oligomerization. We expressed the fragment comprising residues 1–141 and, using gel filtration, determined that it had an apparent molecular mass of ~62 kDa (Supplementary Fig. 2a). Given that coiled coils migrate faster and typically show near double the actual molecular mass, our result was consistent with $NudC^{1–141}$ forming a homodimer. To evaluate if the fragment contains a coiled-coil structure, we used circular dichroism (CD) spectropolarimetry and analyzed the ratio of ellipticities at 222 nm/208 nm. We determined that the 1–141 fragment contains a stretch of

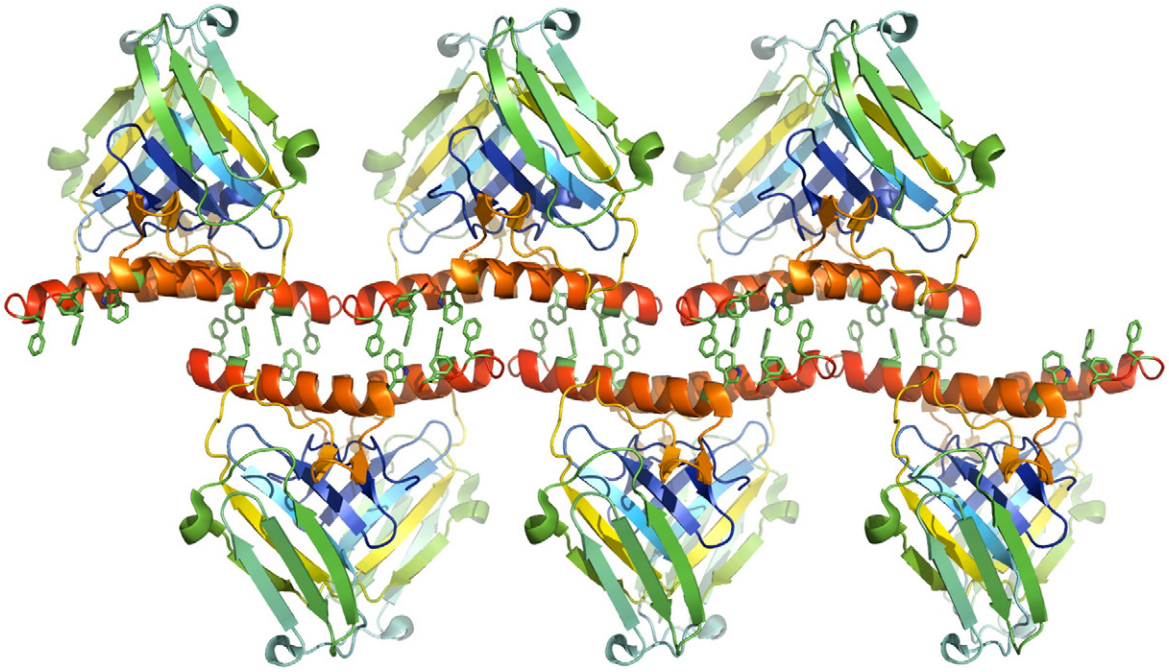

Fig. 5. The principal crystal contacts in the NudCL2 structure showing the assembly of homodimers into a filament *via* a conserved hydrophobic surface. The side chains of Trp113, Phe127, Phe134, and Phe136 are shown in detail, but are not labeled.

approximately 50 amino acids that form a coiled-coil structure, with the remainder forming a random coil (Supplementary Fig. 2b). Theoretical coiled-coil prediction[73] suggests that the sequence between residue 50 and residue 135 has a propensity to form a coiled coil, but with discontinuity at Pro102. We conclude that NudC is a dimer, with the coiled-coil motif (most likely parallel with and encompassing amino acids 50–100) mediating dimerization.

We also evaluated the molecular masses of hNudCL and mNudCL2 in solution using gel filtration. Both proteins behaved as dimers (data not shown). Given sequence similarities between the two proteins, as well as structure prediction, we hypothesize that dimerization in the NudCL subfamily is mediated by its N-terminal coiled-coil motif, in a manner analogous to hNudC. In the case of NudCL2, our data are consistent with the crystal structure and suggest that dimerization occurs through domain swapping.

Chaperone activity of mammalian NudC proteins

The structures of the CS domains in the NudC family bear a distinct similarity to those found in small heat shock chaperones such as p23 and Hsp20, suggesting that NudC proteins may play a similar role in eukaryotic physiology. It should be noted here that some of the CS-domain-containing proteins have been shown to function as Hsp90 cochaperones, but may also show intrinsic chaperone activity independent of Hsp90. Interestingly, experimental evidence supporting both such functions for the NudC family has been published. Specifically, the *C. elegans* NudC homolog NUD-1 has been shown to exhibit chaperone activity *in vitro*, preventing the aggregation of citrate synthase and luciferase.[44] Human NudC has been implicated in Hsp90-mediated pathways, resulting in stabilization of Lis1, and was shown to have intrinsic chaperone activity *in vitro*, preventing aggregation of citrate synthase.[40] Similar observations (i.e., interaction with Hsp90 and Lis1 stabilization) were reported for NudCL2, although it was not established if this paralogue has *in vitro* chaperone activity.[26] The human NudCL was implicated in the stabilization of the dynein intermediate chain through an unknown mechanism.[74] Finally, the *Ar. thaliana* homologue of NudC, BOBBER1, was shown to be a heat shock protein by preventing the thermal aggregation of malate dehydrogenase (MDH); it is also required for development and thermotolerance.[75] In view of these results, we decided to reassess the *in vitro* chaperone activities of all three mammalian NudC family members by monitoring the aggregation of luciferase and citrate synthase using light scattering.

As expected, full-length hNudC clearly displayed chaperone activity and suppressed the aggregation of both luciferase and citrate synthase at ~50% level (Fig. 6). We then took advantage of our knowledge of the structure of hNudC to investigate what structural requirements are necessary for the observed activity. To that end, we tested several hNudC variants, including $hNudC^{1–274}$, which lacks only the unstructured C-terminal tail; $hNudC^{158–274}$ (i.e., the isolated CS domain); $hNudC^{158–331}$, comprising the CS domain and the C-terminal tail; and $hNudC^{1–141}$, which constitutes the dimerization domain. The $hNudC^{1–274}$ variant exhibited chaperone activity similar to that of the wild-type protein. In contrast, the isolated hNudC CS domain ($hNudC^{158–274}$), $hNudC^{158–331}$, and $hNudC^{1–141}$ were unable to

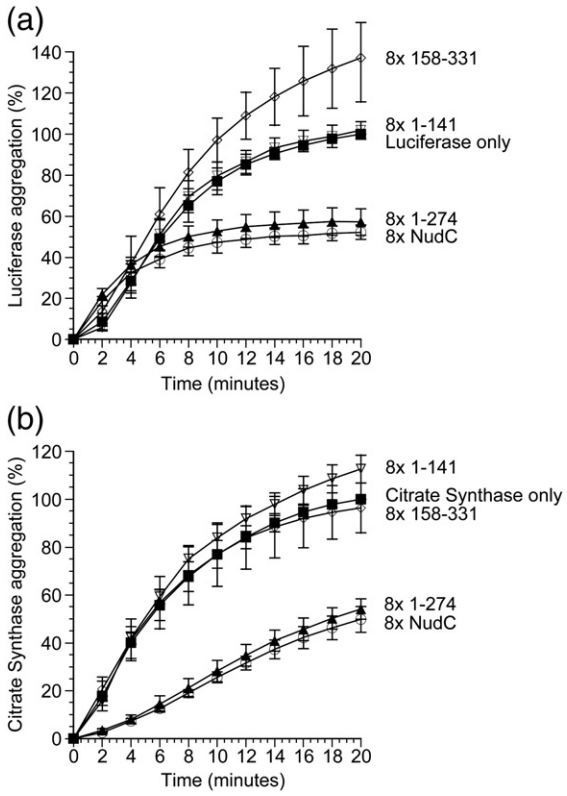

Fig. 6. Dimerization is required for the chaperone activity of NudC. (a) Luciferase (0.1 μM; filled squares) was incubated at 42 °C for 20 min in the presence and in the absence of 0.8 μM NudC (open circles), construct 1–274 (filled triangles), construct 158–331 (open diamonds), and construct 1–141 (open inverted triangles). Aggregation was measured by light scattering at 370 nm. Data represent the average of three independent trials and are expressed as the percent maximum aggregation of luciferase at 20 min with ±mean standard deviation. (b) citrate synthase (0.15 μM; filled squares) was incubated at 44 °C for 20 min in the presence and in the absence of 1.2 μM NudC (open circles), construct 1–274 (filled triangles), construct 158–331 (open diamonds), and construct 1–141 (open inverted triangles). Aggregation was measured and calculated as described in (a). All NudC concentrations were based on the monomeric form.

suppress the aggregation of any of the two substrates (Fig. 6; data not shown). Thus, it appears that dimerization, but not the C-terminal conserved tail, is essential for the chaperone activity.

Next, we investigated if analogous intrinsic chaperone activity could be detected for hNudCL and mNudCL2 (Figs. 7 and 8). As expected, hNudCL displayed such activity, resulting in an essentially complete suppression of aggregation for both protein targets using the same molar concentration as hNudC. In contrast, mNudCL2 displayed inconsistent results, suppressing ~70% of luciferase aggregation, but with no impact on the aggregation of citrate synthase. Because of this substrate discrepancy, we decided to use SDS-PAGE as a secondary readout to monitor the aggregation of luciferase and citrate synthase after the incubation of these proteins with target chaperones.[76] This assay allows for the quantification of the suppression of protein precipitation, but not for the detection of soluble aggregates. Addition of mNudCL2 resulted in a small increase in the concentration of citrate synthase in the supernatant compared with the control, while luciferase was found exclusively in the pellet fraction. In contrast, and in agreement with light-scattering data, hNudCL completely suppressed the aggregation of both luciferase and citrate synthase, with both proteins found after incubation exclusively in the supernatant.

Finally, we used a third well-known chaperone substrate, MDH,[77] and monitored the aggregation by SDS-PAGE (Supplementary Fig. 3). As before, hNudCL completely suppressed the aggregation of MDH, resulting in its localization solely to the soluble supernatant fraction. Neither mNudCL2 nor the negative control hNudC$^{158–331}$ suppressed aggregation. True chaperones are capable of recognizing and interacting with a broad range of nonnative misfolded protein, rather than only specific ones.[78,79] In this regard, hNudC and hNudCL both act consistently as molecular chaperones in suppressing protein aggregation across multiple substrates. Although it could be argued that the ability of NudC

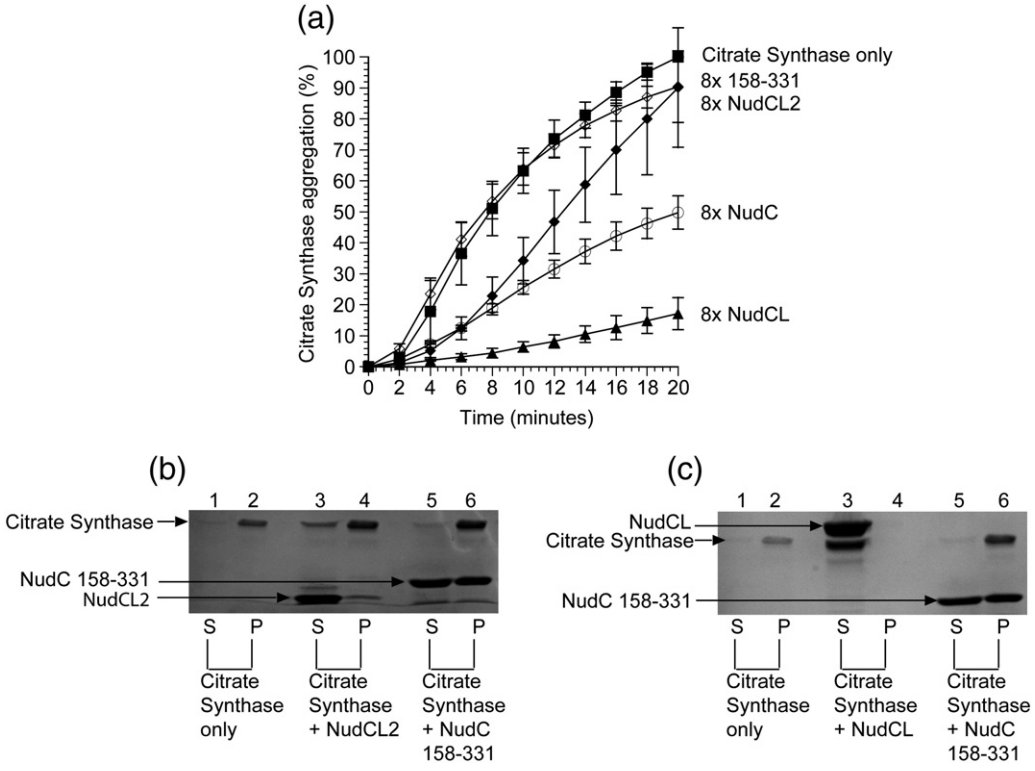

Fig. 7. Suppression of citrate aggregation by NudC proteins. (a) CS (0.15 μM, filled squares) was incubated at 44 °C in the presence and in the absence of 1.2 μM NudC (open circles), NudCL2 (closed diamonds), NudCL (filled triangles), and the negative control NudC construct 158–331 (negative control; open diamonds). Data represent the average of 3 independent trials and are expressed as the percent maximum aggregation of citrate synthase at 20 min with ± mean standard deviation. (b) Lanes 1, 3, and 5 represent the soluble fractions. Lanes 2, 4, and 6 are the insoluble fractions. Lanes 1 and 2 consist of 1.6 μM citrate synthase by itself. Lanes 3 and 4 consist of 12.8 μM NudCL2 with 1.6 μM citrate synthase. Lanes 5 and 6 represent the negative control, 12.8 μM NudC construct 158–331 (negative control) and 1.6 μM citrate synthase. (c) Lanes 1, 3 and 5 represent the soluble fractions and lanes 2, 4, and 6 represent the insoluble fractions. Lanes 1 and 2 consist of 1.6 μM citrate synthase only. Lanes 3 and 4 include 12.8 μM NudCL with 1.6 μM citrate synthase. Lanes 5 and 6 contain 12.8 μM NudC construct 158–331 and 1.6 μM citrate synthase. All NudC concentrations assumed a monomeric state.

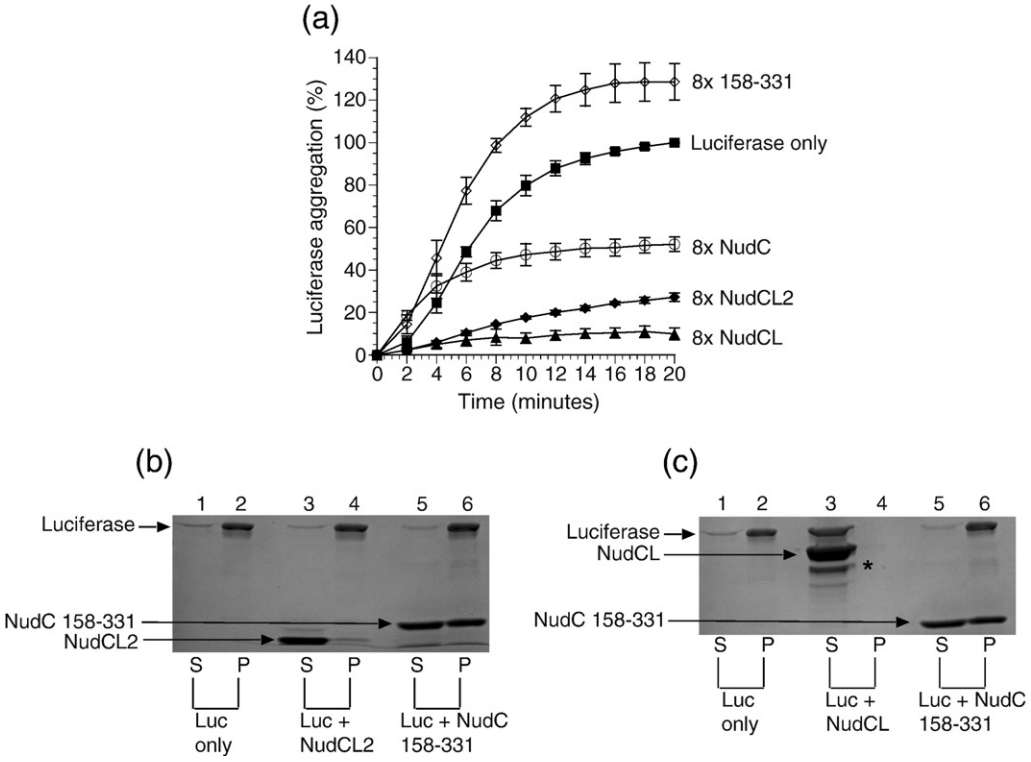

Fig. 8. Suppression of luciferase aggregation by NudC proteins. (a) Luciferase (0.1 μM; filled squares) was incubated at 42 °C in the presence and in the absence of 0.8 μM NudC (open circles), NudCL (filled triangles), NudCL2 (closed diamonds), and NudC construct 158–331 (negative control; open diamonds). Data represent the average of three independent trials and are expressed as the percent maximum aggregation of luciferase at 20 min with ±mean standard deviation. (b) Lanes 1, 3, and 5 represent soluble fractions. Lanes 2, 4, and 6 represent insoluble fractions. Lanes 1 and 2 consist of 0.82 μM luciferase by itself. Lanes 3 and 4 consist of 6.56 μM NudCL2 with 0.82 μM luciferase. Lanes 5 and 6 represent 6.56 μM NudC construct 158–331 (negative control) and 0.82 μM luciferase. (c) Lanes 1, 3, and 5 represent the soluble fractions, and lanes 2, 4, and 6 represent the insoluble fractions. Lanes 1 and 2 consist of 0.82 μM luciferase only. Lanes 3 and 4 include 6.56 μM NudCL with 0.82 μM luciferase. Lanes 5 and 6 contain 6.56 μM NudC construct 158–331 and 0.82 μM luciferase. Asterisk represents a degradation product of NudCL. All NudC concentrations assume a monomeric state.

and NudL to suppress protein aggregation *in vitro* may be due to nonspecific interactions with misfolded substrates, we find this unlikely, as several laboratories now have reported chaperone activity for quite a few different NudC homologs using various chaperone assays with a variety of misfolded substrates.[40,44,75] These assays are well-established for classifying small heat shock chaperones.[80–82] The mNudCL2 protein, however, behaves differently, exhibiting only some activity in the luciferase assay; even then, the results were not reproducible across multiple substrate readouts.

Many proteins act as chaperones in suppressing the protein aggregation of misfolded substrates, but also perform other functions. For example, calreticulin, torsinA, and Hsp90 are involved in nuclear export, maintenance of the nuclear envelope cytoskeletal structure, and cargo loading of dynein, respectively, but all have chaperone-like activities.[83–87] The physiological role of NudC chaperone activity has yet to be elucidated; prior studies have suggested a possible role in protein stabilization, as the absence of NudCL or NudC results in dynein light chain aggregation or lower levels of NudF, respectively.[18,25] Thus, it is possible that NudC and NudCL might be interacting with certain members of the Lis1/dynein complex for stabilization. Regardless, future studies are needed to confirm the role of NudC chaperone activity as it relates to its normal cellular function.

NudC proteins do not interact with Lis1 *in vitro*

CS domains appear to occur predominantly in proteins with chaperone or cochaperone activities, or in proteins that recruit Hsp90 to regulate macromolecular assemblies. It is therefore surprising that the mammalian NudC proteins have been implicated in direct interactions with Lis1 (a WD40 family member), which has no relationship to any chaperone.[19,39,41] Given this apparent inconsistency, we decided to reevaluate if such binary interactions

can be observed *in vitro*. We used bacterially expressed NudC proteins and sf9-expressed human Lis1, both of which are folded correctly, as shown by biophysical and crystallographic studies.[11] As a positive control, we used recombinant Ndel1$^{58–169}$, which is well-documented to bind Lis1 with a dissociation constant (K_d) of ~0.3 μM.[11,16] In isothermal titration calorimetry (ITC) experiments, we were easily able to reproduce the Lis1/Ndel1 interactions, while none of the three NudC proteins appeared to interact with Lis1, as inferred from lack of enthalpy change (Fig. 9a). Because ITC experiments detect only enthalpy changes and since entropy-driven effects may be overlooked, we also conducted canonical pull-down experiments. They confirmed that NudC proteins do not form binary complexes with Lis1 (Fig. 9b).

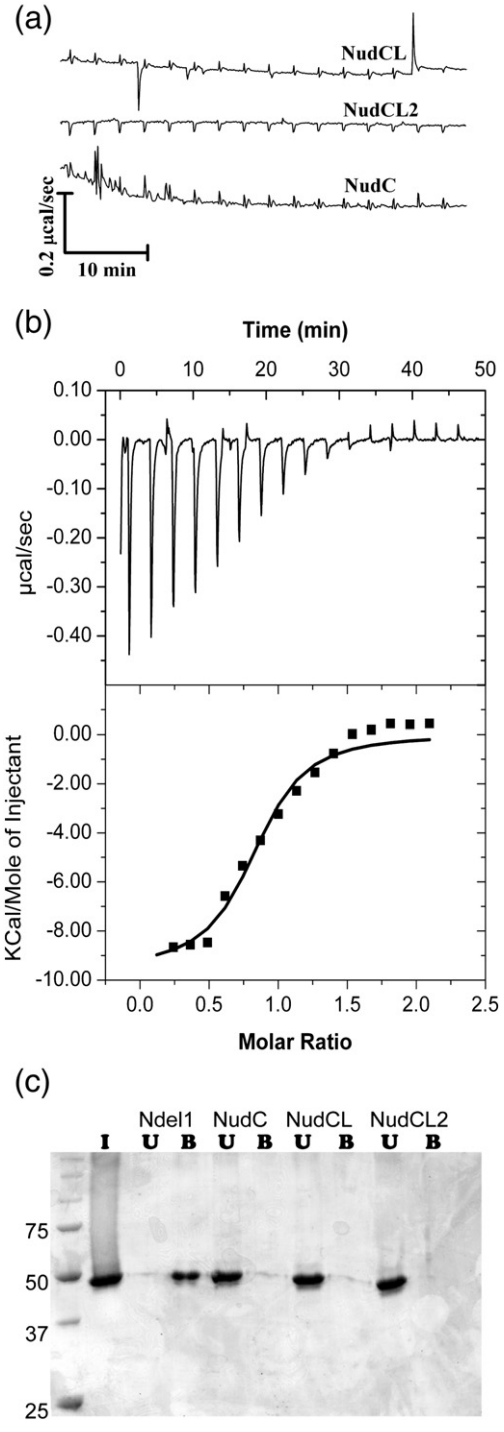

Fig. 9. The NudC proteins do not form binary complexes with Lis1. (a) Raw calorimetric titration data for the three NudC proteins titrated against Lis1 (see Materials and Methods) showing no enthalpy change. (b) Positive control showing the titration curve of Lis1 against Ndel1, a known partner of Lis1. An ITC profile of the interaction of Ndel1 with Lis1 is shown in the upper panel, and individual dissipated heats plotted against the molar ratio of interacting proteins are shown in the lower panel. The data were fitted with a "one-set-of-sites model" shown as a continuous line on the lower panel. The best fit resulted in $K_a = 6.4 \times 10^5\ M^{-1}$, $n = 0.83$, and $\Delta H = -9.5$ kcal/mol dimer. (c) Pull-down experiments showing a binary interaction of Lis1 with Ndel1 (see Materials and Methods) and no interaction with any of the NudC proteins. I, input; U, unbound (i.e., flow-through); B, bound.

Concluding Remarks

The biological importance of the NudC family of proteins is undisputed. The high level of amino acid conservation in each of the three subfamilies and the ubiquitous presence of the proteins in all tissues and cells examined both during development and in adult life are all consistent with a critical function that these proteins play in cell physiology, most probably in mitotic cell division and proliferation. However, the precise mechanism by which these proteins function is not known. Two hypotheses were particularly intriguing. First, the genetic link to the fungal NudC and therefore to other proteins of the Nud family strongly suggested a functional coupling to dynein regulation. This has inspired a number of investigators to look at the direct interactions of NudC with Lis1.[19,39,41] Second, the expected similarity of the NudC globular domain to the CS domain of p23 and Hsp20 suggested an alternative role for NudC family members as chaperones and/or cochaperones. In this article, we explored both these possibilities through an analysis of the structural features of NudC itself, NudCL, and NudCL2; their ability to bind Lis1 *in vitro*; and their performance in *in vitro* chaperone assays.

First, it is important to note that both NudC and NudCL share the overall molecular architecture. They are homodimeric proteins with a modular structure: a coiled-coil motif stretching over a fragment ~50–70 residues long in the N-terminal

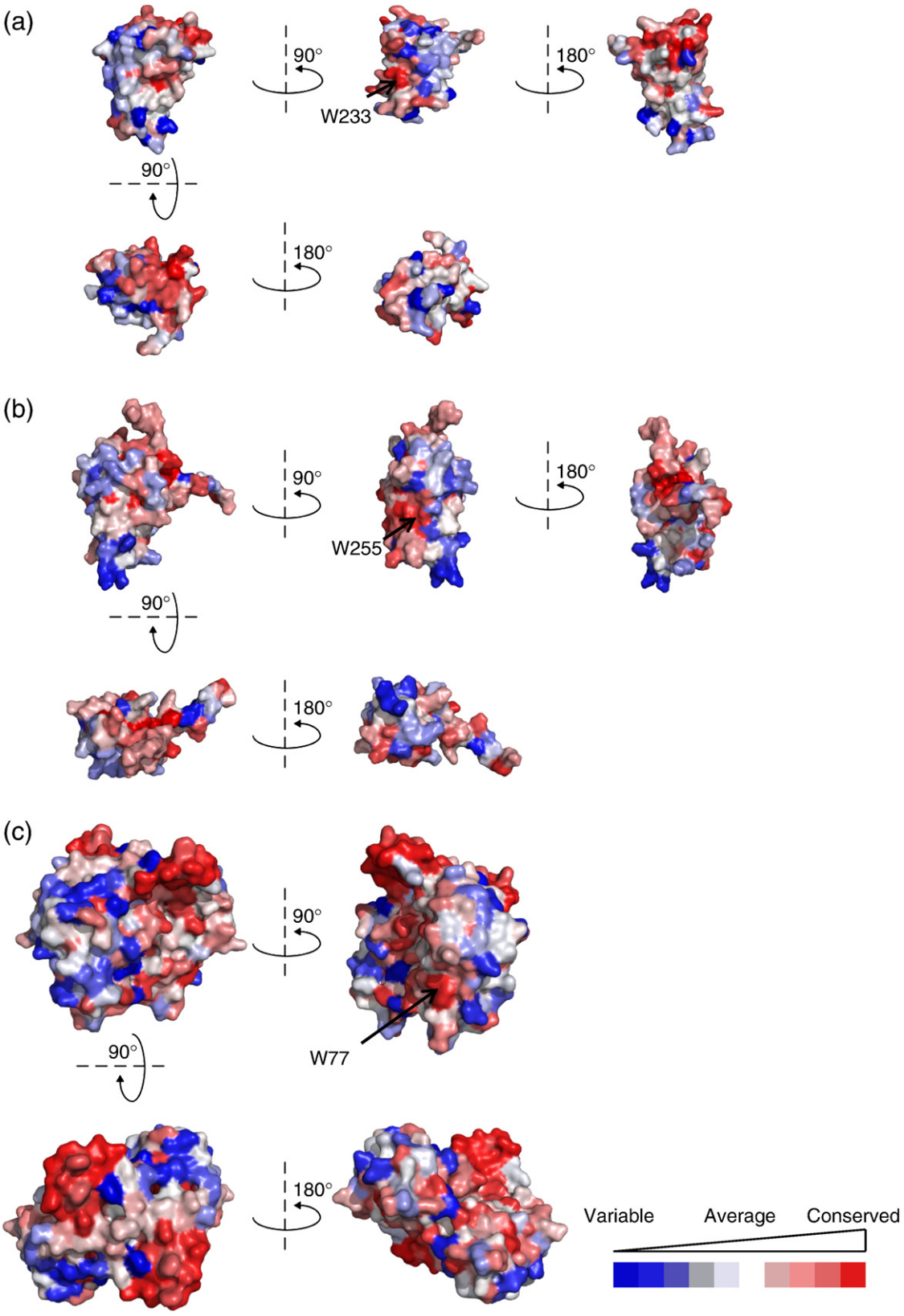

Fig. 10 (*legend on next page*)

section constitutes the dimerization module, followed by a flexible linker, a CS domain, and, finally, two highly conserved α-helices separated by a short loop, which do not seem to interact with the CS domain. This conserved architecture of the two proteins suggests possible functional redundancy, although amino acid sequence identity between the two is relatively low. It is important to realize that these molecules are obligate dimers, and biological function may well be dependent on dimerization. Thus, studies of isolated fragments, such as CS domains alone, are prone to misinterpretation if the oligomeric structure is not taken into account. A particularly intriguing feature of both NudC and NudCL is the C-terminal α-helical element. An extremely high amino acid sequence conservation of this fragment suggests that this is a very specific targeting module that interacts with an as yet unidentified protein. There are other examples of similar architecture where a stable helix (not otherwise associated with a tertiary domain) is essential for the formation of a binary complex. One such example is the human Rho GTPase guanine dissociation inhibitor (Rho GDI), which contains a globular domain and two flexible α-helices (which do not interact with the former but attain an ordered structure only in complex with the target Rho GTPase).[88,89] However, it is possible that this element can only function within a homodimeric ensemble.

The NudCL2 protein is a good example of the danger of misinterpretations based on sequence analysis alone. While the sequence suggests that this protein is similar to NudC/NudCL, albeit without the N-terminal dimerization module and the linker, the crystal structure reveals a different story: the protein is also an obligate dimer, but dimerization occurs due to domain swapping involving the last β-strand and the C-terminal helix, rather than an element extraneous to the CS domain. Again, this architecture must be taken into account when one designs mutants and deletion variants for functional studies. For example, dissecting NudCL2 into fragments to assess their binding abilities most likely destroys the protein's integrity and results in unfolded denatured fragments.

The crystal structures cannot reveal precise cellular functions, but can provide useful hints. The presence of CS domains in all NudC homologues is consistent with a chaperone or cochaperone role. Such domains, while ubiquitous, have not been shown to be involved in any signaling events *via* specific protein–protein interactions.

Intrinsic *in vitro* chaperone activity has been reported for the *C. elegans* NudC homologue[44] and for the human NudC,[40] and chaperone or cochaperone functions have been suggested for both NudCL and NudCL2.[25,26] We were able to confirm that both NudC and NudCL, but not NudCL2, are able to suppress the aggregation of a range of protein targets *in vitro*, and we find that the chaperone activities are dependent on the dimeric architecture of these proteins, but not on the presence of the highly conserved C-terminal fragment. It is therefore surprising that an L279P mutant of hNudC, where the mutation is located within the C-terminal fragment, was recently reported to lower the chaperone activity.[40] One possible explanation is that the mutated C-terminus somehow interferes with the remainder of the protein. It is also important to note that the dimeric structures of NudC and NudCL do not exclude the possibility that these proteins may interact with Hsp90 *via* the CS domain and/or C-terminal helices.

In contrast, the NudCL2 protein presents a very different picture. It is unlikely to function in the same way as NudC or NudCL because of its different molecular architecture. However, the conserved solvent-exposed hydrophobic surface that includes Trp113, Phe127, Phe134, and Phe136 contacts strongly suggests potential for protein–protein interactions. Furthermore, it is able to form filaments in the crystal structure, indicating that it may form low-affinity polymers or indeed interact with unstable or unfolded proteins similarly to chaperones.

The molecular mechanisms of intrinsic chaperones are often elusive because identifying functional surfaces is difficult. Given that all three NudC subfamilies may function as chaperones, we wondered if surface sequence conservation might reveal some clues to the mechanism. Interestingly (Fig. 10), we found that each subfamily contains some conserved patches, with one patch in the same topological location in all three subfamilies. This patch contains a single amino acid that is solvent-exposed and completely conserved throughout all NudC proteins: Trp233 (NudC), Trp255 (NudCL), and Trp77 (NudCL2). Further work will be necessary to clarify if this pattern of evolutionary conservation is related to functional properties.

Finally, we tested if the NudC proteins bind Lis1. We took advantage of structural information and used insect-cell-derived Lis1 (known to fold properly) and full-length homodimeric forms of

Fig. 10. Sequence conservation, calculated as described in Materials and Methods, was mapped onto the (a) hNudC, (b) mNudCL, and (c) mNudCL2 (dimer) protein surfaces. The level of conservation is depicted on a color scale from blue (least conserved) to red (most conserved). The mNudCL structure and chain A of mNudCL2 were aligned to hNudC and rotated as indicated. The only fully invariant amino acid, based on sequence alignment and topology, is a tryptophan indicated by an arrow in each case.

recombinant NudC, NudCL, and NudCL2 proteins. Using both ITC and pull-down assays, we show conclusively that no binary complexes are formed by any of these proteins with Lis1. We also tested if NudC interacts with the Lis1/Ndel1 complex and obtained equally negative data (data not shown). The original observation of NudC/Lis1 interaction was based on a yeast two-hybrid screen and a pull-down assay using a glutathione *S*-transferase (GST)/NudC fusion as bait and rat Nb2T cell extracts.[39] It was further shown that NudC and Lis1 colocalize and can be detected using coimmunoprecipitation.[39,41] Similarly, the fungal (*Aspergillus*) NudF protein was identified as a NudC interactor through the yeast two-hybrid system.[19] None of these studies involved a rigorous biophysical assay of binary interaction using recombinant proteins that were shown to be properly folded. It is possible that one and more of the NudC family members associate in the cell with larger complexes containing Lis1, or that the interaction is mediated by an as yet uncharacterized protein; however, based on our experimental data, direct binding is very unlikely.

Structural characterization of the NudC family will help in further elucidating their cellular functions.

Materials and Methods

Clones, protein expression, and purification

The human *nudC* clone was purchased from the American Type Culture Collection. The expression vectors were constructed using Gateway™ (Invitrogen) technology and two templates [i.e., pDESTHisMBP, containing a His_6-tagged maltose binding protein (MBP), and pDEST15, containing GST as the N-terminal fusion tag]. The fusion tag was followed by the tabacco etch virus (TEV) protease cleavage site and a Ser_4 spacer to improve proteolytic digestion. The vectors used were pDESTHisMBP-1 ($NudC^{1–331}$), pDESTHisMBP-2 ($NudC^{143–331}$), pDESTHisMBP-3 ($NudC^{158–331}$), pDESTHisMBP-4 ($NudC^{158–274}$), and pDESTHisMBP-5 ($NudC^{162–274}$), as well as pDEST15-6 ($NudC^{1–141}$), pDEST15-7 ($NudC^{56–141}$), and pDEST15-8 ($NudC^{1–331}$).

An expression-ready construct, encoding a full-length mouse NudCL2 preceded by an expression–purification tag MGSDKIHHHHHH and a TEV protease cleavage site, was kindly provided by the Joint Center for Structural Genomics. Human NudCL and Lis1 were amplified by Phusion polymerase (New England Biolabs) using reverse-transcribed total human reference RNA (Clontech) as template for PCR. The cDNA fragments obtained were cloned into a pHisParallel vector containing a His_6-tag and a TEV cleavage site.[90] $Ndel^{58–167}$ was amplified from full-length cDNA[16] and also cloned into a pHisParallel vector.

All hNudC variants and hNudCL were expressed in *Escherichia coli* BL21(DE3) RIPL (Stratagene, Inc.) using routine protocols, with minor variations. Briefly, expression was carried out in terrific broth with ampicillin and chloramphenicol, following induction at 37 °C with 0.5 mM isopropyl β-D-1-thiogalactopyranoside, for 16 h at 18 °C. Cells were harvested by centrifugation and lysed by sonication. All proteins were purified using standard Ni-NTA or GST affinity chromatography. Recombinant TEV was used to cleave the His_6-MBP, GST, or His_6-tag, followed by gel filtration. Pure protein fractions were pooled together and concentrated to ~5–15 mg/ml for use in NMR analysis, biophysical studies, and crystallization. The mNudCL2 protein was expressed and purified in a similar manner, except that BL21 cells were used and the expression was induced by the addition of L-arabinose to a final concentration of 0.3%.

To generate SeMet-labeled hNudC samples, we expressed the variants in *E. coli* B834 cells using the autoinduction medium containing SeMet. The cultures were grown for 4.5 h at 37 °C, followed by ~16 h at 20 °C and another 24 h at 10 °C. The proteins were purified as described above.

Human Lis1 was expressed in Sf9 cells and purified to homogeneity, as described previously.[11] The rat Ndel1 fragment encompassing residues 58–167 was expressed in *E. coli* and purified as described elsewhere.[16]

Crystallography

Because wild-type $NudC^{158–274}$ did not yield X-ray-quality crystals, we designed five variants: K227A,E229A, E230A; K267A,K268A; K250A,E252A; E236A,K239A; and K194A,K196A. The proteins were expressed and purified as described above. The wild-type and mutant proteins were screened with the Wizard II crystallization matrix (Emerald Biosystems) using reservoirs containing the screen solution. The double mutant E236A,E239A yielded diffraction-quality crystals from 25% polyethylene glycol 3350, $Na(CH_3COO)$ (pH 4.5), and 0.1 M $LiSO_4$, and crystallization of SeMet-labeled samples was optimized starting from these conditions. Single-wavelength anomalous diffraction data collection at a Se absorption peak wavelength of 0.97928 Å was carried out at SER-CAT 22-ID beamline at Advanced Photon Source (Argonne National Laboratory, Chicago, IL). Data were processed and scaled using HKL2000.[69] The crystals assumed a monoclinic $P2_1$ symmetry with unit cell dimensions of $a = 66.7$ Å, $b = 51.8$ Å, $c = 92.9$ Å, and $\beta = 90.6°$. The positions of Se atoms were obtained using SHELXD.[91] The experimental phases of the anomalous substructure were refined using SHELXE.[92]

The model was built automatically using ARP/wARP,[93] which built 527 out of 580 residues. Crystallographic refinement was completed using Refmac5[94] from the CCP4 suite and Phenix.[95] Programs 'O'[96] and Coot[97] were used for model display and manual model improvement. The refinement converged to an R-factor of 17.2% with an R_{free} of 20.6%. The final model contains five copies of NudC molecule residues 158–274. Serine residue 274 in chains C and D is not well ordered and therefore was removed from the final model. All copies of the molecule contain extra electron density for serine amino acids that were inserted into the plasmid between the cloning sites for NudC and TEV proteinase for faster cleavage during protein purification. For structure validation, we used MolProbity[98] and PROCHECK.[99]

Surface sequence conservation

Surface sequence conservation was analyzed using Consurf.[100,101] Homologues were automatically chosen from the UniRef90 database using default parameters and aligned with the MAFFT-L-INS-i algorithm.

Nuclear magnetic resonance

To produce ^{15}N-labeled samples, we expressed the respective variants in minimal media, with $(^{15}NH_4)_2SO_4$ as the sole source of nitrogen. The media were enhanced by the addition of labeled BioExpress (Cambridge Isotope Laboratories). Samples were purified using the procedure described above for wild-type proteins. NMR spectra for various CS domain constructs were collected using a Varian Inova 500-MHz spectrometer at 25 °C. The NMR samples containing ^{15}N-labeled hNudC fragments 143–331, 158–331, 158–274, and 162–274 were prepared in Tris buffer (pH 7.5) and 150 mM NaCl. The HSQC and ^{15}N{^{1}H} heteronuclear NOE experiments for hNudC$^{158–331}$ were also collected using a Bruker Avance III 800-MHz spectrometer at 25 °C. For the analysis of hNudC$^{56–141}$, we conducted HSQC and ^{15}N{^{1}H} heteronuclear NOE experiments using a Varian Inova 500-MHz spectrometer at 25 °C. For these experiments, 1 mM ^{15}N-labeled protein sample was prepared in 50 mM phosphate buffer (pH 6.5) and 50 mM NaCl.

Analytical gel filtration

Analytical gel filtration was carried out using Superdex 7510/300 GL (GE Healthcare) to determine the size and molecular mass of NudC proteins. By comparing its elution volume with those of known protein standards, we determined the molecular mass of NudC. The standard proteins used for size determination include albumin (molecular mass, 67 kDa), ovalbumin (chicken; molecular mass, 44 kDa), chymotrypsinogen A (molecular mass, 25 kDa), and ribonuclease A (molecular mass, 13.7 kDa).

CD spectropolarimetry

CD spectra were recorded on an AVIV Model 215 CD spectropolarimeter (AVIV Instruments, Lakewood, NJ) equipped with thermoelectric temperature control. Data were recorded from 190 nm to 260 nm in benign buffer [150 mM NaCl and 50 mM Tris buffer (pH 8.0)] and in buffer diluted 1:1 (vol/vol) with trifluoroethanol.

Chaperone assays

Citrate synthase and MDH were obtained from Sigma. Luciferase was purchased from Promega. Measurement of citrate synthase and luciferase aggregation was performed as described previously.[44] Briefly, citrate synthase or luciferase was heated for 20 min in the presence and in the absence of full-length NudC or its constructs, and light scattering was measured with excitation and emission at 370 nm with a 2.5-nm slit width on a PerkinElmer LS55 spectrofluorometer. The aggregation of luciferase, citrate synthase, and MDH was detected by SDS-PAGE, followed by Coomassie staining, as previously reported[76] by incubating luciferase, citrate synthase, or MDH for 1 h in the presence and in the absence of NudCL, NudCL2, or the negative control NudC$^{158–331}$. Reactions were then spun down in a microcentrifuge at 13,000 rpm to separate the insoluble pellet from the soluble fraction. The pellet was then resuspended in a volume equal to the supernatant, and proteins were separated by SDS-PAGE and visualized by Coomassie staining.

Pull-down experiments

The three NudC family proteins and Ndel$^{158–167}$ were each dialyzed against a solution containing 0.1 M $NaHCO_3$ and 0.5 M NaCl, and were covalently linked to CNBr-activated Sepharose (Bio-Rad) according to the manufacturer's instructions using 5 mg of protein per milliliter of Sepharose. Lis1 was dialyzed against the buffer containing 50 mM Tris (pH 8.0), 150 mM NaCl, and 5 mM mercaptoethanol, and diluted with the same buffer to a final concentration of 0.5 mg/ml. Lis1 (250 μl) was added to 50 μl of Sepharose with covalently immobilized NudC proteins or Ndel1 and incubated for 1 h at room temperature. Unbound fraction was recovered, and beads were washed three times and boiled in sample buffer to release bound Lis1. Bound and unbound fractions were analyzed on Coomassie-stained SDS-PAGE gels.

Isothermal titration calorimetry

ITC was performed at 25 °C using a Microcal ITC-200 calorimeter (MicroCal, Northampton, MA). Protein samples were dialyzed against a buffer containing 20 mM Tris, 200 mM NaCl, and 5 mM 2-mercaptoethanol prior to the experiment. Contents of the sample cell were stirred continuously at 300 rpm during the experiment. A typical titration of Lis1 involved 18–20 injections of Ndel1 or one injection of the NudC family proteins (0.3–0.9 mM, 2 μl, 3-min intervals) into a sample cell containing 0.2 ml of Lis1 (70–110 μM). The baseline-corrected data were analyzed with Microcal Origin 5.0 software to determine the enthalpy (ΔH), entropy (S), association constant (K_a), and stoichiometry of binding (N) by fitting to the association model for a single set of identical sites.

Accession numbers

The atomic coordinates and structure factors for the hNudC CS domain structure have been deposited under PDB accession number 3QOR.

Supplementary materials related to this article can be found online at doi:10.1016/j.jmb.2011.04.018

Acknowledgements

This research was supported by a grant from the National Institutes of Health (NS036267) to Z.S.D. We thank Ms. Natalya Olekhnovich for technical assistance and Dr. Jeff Elena for assistance with

NMR experiments. The use of Advanced Photon Source was supported by the US Department of Energy, Office of Science, Office of Basic Energy Sciences, under contract no. W-31-109-Eng-38. Supporting institutions of SER-CAT may be found at http://www.ser-cat.org/members.html.

References

1. Morris, N. R. (1975). Mitotic mutants of *Aspergillus nidulans*. *Genet. Res.* **26**, 237–254.
2. Xiang, X., Beckwith, S. M. & Morris, N. R. (1994). Cytoplasmic dynein is involved in nuclear migration in *Aspergillus nidulans*. *Proc. Natl Acad. Sci. USA*, **91**, 2100–2104.
3. Xiang, X., Osmani, A. H., Osmani, S. A., Xin, M. & Morris, N. R. (1995). NudF, a nuclear migration gene in *Aspergillus nidulans* is similar to the human *LIS-1* gene required for neuronal migration. *Mol. Biol. Cell.* **6**, 297–310.
4. Willins, D. A., Xiang, X. & Morris, N. R. (1995). An alpha tubulin mutation suppresses nuclear migration mutations in *Aspergillus nidulans*. *Genetics*, **141**, 1287–1298.
5. Morris, N. R., Xiang, X. & Beckwith, S. M. (1995). Nuclear migration advances in fungi. *Trends Cell. Biol.* **5**, 278–282.
6. Beckwith, S. M., Roghi, C. H. & Morris, N. R. (1995). The genetics of nuclear migration in fungi. *Genet. Eng. (NY)*, **17**, 165–180.
7. Jones, K. L., Gilbert, E. F., Kaveggia, E. G. & Opitz, J. M. (1980). The Miller–Dieker syndrome. *Pediatrics*, **66**, 277–281.
8. Reiner, O., Carrozzon, R., Shen, Y., Wehnert, M., Faustinella, F., Dobyns, W. B. *et al.* (1993). Isolation of a Miller–Dieker lissencephaly gene containing G-protein β-subunits-like repeats. *Nature (London)*, **364**, 717–721.
9. Hattori, M., Adachi, H., Tsujimoto, M., Arai, H. & Inoue, K. (1994). Miller–Dieker lissencephaly gene encodes a subunit of brain platelet-activating factor acetylhydrolase. *Nature (London)*, **370**, 216–218.
10. Morris, N. R. (2000). Nuclear migration. From fungi to the mammalian brain. *J. Cell Biol.* **148**, 1097–1101.
11. Tarricone, C., Perrina, F., Monzani, S., Massimiliano, L., Kim, M. H., Derewenda, Z. S. *et al.* (2004). Coupling PAF signaling to dynein regulation: structure of LIS1 in complex with PAF-acetylhydrolase. *Neuron*, **44**, 809–821.
12. Kardon, J. R. & Vale, R. D. (2009). Regulators of the cytoplasmic dynein motor. *Nat. Rev. Mol. Cell Biol.* **10**, 854–865.
13. Niethammer, M., Smith, D. S., Ayala, R., Peng, J., Ko, J., Lee, M. *et al.* (2000). NUDEL is a novel Cdk5 substrate that associates with LIS1 and cytoplasmic dynein. *Neuron*, **28**, 697–711.
14. Feng, Y., Olson, E. C., Stukenberg, P. T., Flanagan, L. A., Kirschner, M. W. & Walsh, C. A. (2000). LIS1 regulates CNS lamination by interacting with mNudE, a central component of the centrosome. *Neuron*, **28**, 665–679.
15. Yan, X., Li, F., Liang, Y., Shen, Y., Zhao, X., Huang, Q. & Zhu, X. (2003). Human Nudel and NudE as regulators of cytoplasmic dynein in poleward protein transport along the mitotic spindle. *Mol. Cell. Biol.* **23**, 1239–1250.
16. Derewenda, U., Tarricone, C., Choi, W. C., Cooper, D. R., Lukasik, S., Perrina, F. *et al.* (2007). The structure of the coiled-coil domain of Ndel1 and the basis of its interaction with Lis1, the causal protein of Miller–Dieker lissencephaly. *Structure*, **15**, 1467–1481.
17. McKenney, R. J., Vershinin, M., Kunwar, A., Vallee, R. B. & Gross, S. P. (2010). LIS1 and NudE induce a persistent dynein force-producing state. *Cell*, **141**, 304–314.
18. Chiu, Y. H., Xiang, X., Dawe, A. L. & Morris, N. R. (1997). Deletion of nudC, a nuclear migration gene of *Aspergillus nidulans*, causes morphological and cell wall abnormalities and is lethal. *Mol. Biol. Cell*, **8**, 1735–1749.
19. Helmstaedt, K., Laubinger, K., Vosskuhl, K., Bayram, O., Busch, S., Hoppert, M. *et al.* (2008). The nuclear migration protein NUDF/LIS1 forms a complex with NUDC and BNFA at spindle pole bodies. *Eukaryotic Cell*, **7**, 1041–1052.
20. Dawe, A. L., Caldwell, K. A., Harris, P. M., Morris, N. R. & Caldwell, G. A. (2001). Evolutionarily conserved nuclear migration genes required for early embryonic development in *Caenorhabditis elegans*. *Dev. Genes Evol.* **211**, 434–441.
21. Cunniff, J., Chiu, Y. H., Morris, N. R. & Warrior, R. (1997). Characterization of DnudC, the *Drosophila* homolog of an *Aspergillus* gene that functions in nuclear motility. *Mech. Dev.* **66**, 55–68.
22. Moreau, N., Aumais, J. P., Prudhomme, C., Morris, S. M. & Yu-Lee, L. Y. (2001). NUDC expression during amphibian development. *Int. J. Dev. Biol.* **45**, 839–843.
23. Miller, B. A., Zhang, M. Y., Gocke, C. D., De Souza, C., Osmani, A. H., Lynch, C. *et al.* (1999). A homolog of the fungal nuclear migration gene nudC is involved in normal and malignant human hematopoiesis. *Exp. Hematol.* **27**, 742–750.
24. Matsumoto, N. & Ledbetter, D. H. (1999). Molecular cloning and characterization of the human NUDC gene. *Hum. Genet.* **104**, 498–504.
25. Zhou, T., Zimmerman, W., Liu, X. & Erikson, R. L. (2006). A mammalian NudC-like protein essential for dynein stability and cell viability. *Proc. Natl Acad. Sci. USA*, **103**, 9039–9044.
26. Yang, Y., Yan, X., Cai, Y., Lu, Y., Si, J. & Zhou, T. (2010). NudC-like protein 2 regulates the LIS1/dynein pathway by stabilizing LIS1 with Hsp90. *Proc. Natl Acad. Sci. USA*, **107**, 3499–3504.
27. Garcia-Ranea, J. A., Mirey, G., Camonis, J. & Valencia, A. (2002). p23 and HSP20/alpha-crystallin proteins define a conserved sequence domain present in other eukaryotic protein families. *FEBS Lett.* **529**, 162–167.
28. Wang, Q., Li, M., Wang, Y., Zhang, Y., Jin, S., Xie, G. *et al.* (2008). RNA interference targeting CML66, a novel tumor antigen, inhibits proliferation, invasion and metastasis of HeLa cells. *Cancer Lett.* **269**, 127–138.
29. Yang, X. F., Wu, C. J., McLaughlin, S., Chillemi, A., Wang, K. S., Canning, C. *et al.* (2001). CML66, a broadly immunogenic tumor antigen, elicits a humoral immune response associated with remission of

chronic myelogenous leukemia. *Proc. Natl Acad. Sci. USA*, **98**, 7492–7497.
30. Gocke, C. D., Osmani, S. A. & Miller, B. A. (2000). The human homologue of the *Aspergillus* nuclear migration gene nudC is preferentially expressed in dividing cells and ciliated epithelia. *Histochem. Cell. Biol.* **114**, 293–301.
31. Zhang, M. Y., Huang, N. N., Clawson, G. A., Osmani, S. A., Pan, W., Xin, P. *et al.* (2002). Involvement of the fungal nuclear migration gene nudC human homolog in cell proliferation and mitotic spindle formation. *Exp. Cell Res.* **273**, 73–84.
32. Zhou, T., Aumais, J. P., Liu, X., Yu-Lee, L. Y. & Erikson, R. L. (2003). A role for Plk1 phosphorylation of NudC in cytokinesis. *Dev. Cell*, **5**, 127–138.
33. Aumais, J. P., Williams, S. N., Luo, W., Nishino, M., Caldwell, K. A., Caldwell, G. A. *et al.* (2003). Role for NudC, a dynein-associated nuclear movement protein, in mitosis and cytokinesis. *J. Cell Sci.* **116**, 1991–2003.
34. Nishino, M., Kurasawa, Y., Evans, R., Lin, S. H., Brinkley, B. R. & Yu-Lee, L. Y. (2006). NudC is required for Plk1 targeting to the kinetochore and chromosome congression. *Curr. Biol.* **16**, 1414–1421.
35. Hatakeyama, H., Kondo, T., Fujii, K., Nakanishi, Y., Kato, H., Fukuda, S. & Hirohashi, S. (2006). Protein clusters associated with carcinogenesis, histological differentiation and nodal metastasis in esophageal cancer. *Proteomics*, **6**, 6300–6316.
36. Lin, S. H., Nishino, M., Luo, W., Aumais, J. P., Galfione, M., Kuang, J. & Yu-Lee, L. Y. (2004). Inhibition of prostate tumor growth by overexpression of NudC, a microtubule motor-associated protein. *Oncogene*, **23**, 2499–2506.
37. Hartmann, T. B., Mattern, E., Wiedemann, N., van Doorn, R., Willemze, R., Niikura, T. *et al.* (2008). Identification of selectively expressed genes and antigens in CTCL. *Exp. Dermatol.* **17**, 324–334.
38. Suzuki, S. O., McKenney, R. J., Mawatari, S., Mizuguchi, M., Mikami, A., Iwaki, T. *et al.* (2007). Expression patterns of LIS1, dynein and their interaction partners dynactin, NudE, NudEL and NudC in human gliomas suggest roles in invasion and proliferation. *Acta Neuropathol.* **113**, 591–599.
39. Morris, S. M., Albrecht, U., Reiner, O., Eichele, G. & Yu-Lee, L. Y. (1998). The lissencephaly gene product Lis1, a protein involved in neuronal migration, interacts with a nuclear movement protein, NudC. *Curr. Biol.* **8**, 603–606.
40. Zhu, X. J., Liu, X., Jin, Q., Cai, Y., Yang, Y. & Zhou, T. (2010). The L279P mutation of nuclear distribution gene C (NudC) influences its chaperone activity and lissencephaly protein 1 (LIS1) stability. *J. Biol. Chem.* **285**, 29903–29910.
41. Aumais, J. P., Tunstead, J. R., McNeil, R. S., Schaar, B. T., McConnell, S. K., Lin, S. H. *et al.* (2001). NudC associates with Lis1 and the dynein motor at the leading pole of neurons. *J. Neurosci.* **21**, RC187.
42. Riera, J., Rodriguez, R., Carcedo, M. T., Campa, V. M., Ramos, S. & Lazo, P. S. (2007). Isolation and characterization of nudC from mouse macrophages, a gene implicated in the inflammatory response through the regulation of PAF-AH(I) activity. *FEBS Lett.* **581**, 3057–3062.
43. Yamada, M., Toba, S., Takitoh, T., Yoshida, Y., Mori, D., Nakamura, T. *et al.* (2010). mNUDC is required for plus-end-directed transport of cytoplasmic dynein and dynactins by kinesin-1. *EMBO J.* **29**, 517–531.
44. Faircloth, L. M., Churchill, P. F., Caldwell, G. A. & Caldwell, K. A. (2009). The microtubule-associated protein, NUD-1, exhibits chaperone activity *in vitro*. *Cell Stress Chaperones*, **14**, 95–103.
45. Chen, W. M., Yu, B., Zhang, Q. & Xu, P. (2010). Identification of the residues in the extracellular domain of thrombopoietin receptor involved in the binding of thrombopoietin and a nuclear distribution protein (human NUDC). *J. Biol. Chem.* **285**, 26697–26709.
46. Pang, S. F., Li, X. K., Zhang, Q., Yang, F. & Xu, P. (2009). Interference RNA (RNAi)-based silencing of endogenous thrombopoietin receptor (Mpl) in Dami cells resulted in decreased hNUDC-mediated megakaryocyte proliferation and differentiation. *Exp. Cell Res.* **315**, 3563–3573.
47. Tang, Y. S., Zhang, Y. P. & Xu, P. (2008). hNUDC promotes the cell proliferation and differentiation in a leukemic cell line *via* activation of the thrombopoietin receptor (Mpl). *Leukemia*, **22**, 1018–1025.
48. Zhang, Y. P., Tang, Y. S., Chen, X. S. & Xu, P. (2007). Regulation of cell differentiation by hNUDC *via* a Mpl-dependent mechanism in NIH 3T3 cells. *Exp. Cell Res.* **313**, 3210–3221.
49. Wei, M. X., Yang, Y., Ge, Y. C. & Xu, P. (2006). Functional characterization of hNUDC as a novel accumulator that specifically acts on *in vitro* megakaryocytopoiesis and *in vivo* platelet production. *J. Cell. Biochem.* **98**, 429–439.
50. Pan, R. M., Yang, Y., Wei, M. X., Yu, X. B., Ge, Y. C. & Xu, P. (2005). A microtubule associated protein (hNUDC) binds to the extracellular domain of thrombopoietin receptor (Mpl). *J. Cell. Biochem.* **96**, 741–750.
51. Riera, J. & Lazo, P. S. (2009). The mammalian NudC-like genes: a family with functions other than regulating nuclear distribution. *Cell. Mol. Life Sci.* **66**, 2383–2390.
52. Lupas, A., Van Dyke, M. & Stock, J. (1991). Predicting coiled coils from protein sequences. *Science*, **252**, 1162–1164.
53. Srivastava, M., Begovic, E., Chapman, J., Putnam, N. H., Hellsten, U., Kawashima, T. *et al.* (2008). The *Trichoplax* genome and the nature of placozoans. *Nature*, **454**, 955–960.
54. Kajan, L. & Rychlewski, L. (2007). Evaluation of 3D-Jury on CASP7 models. *BMC Bioinf.* **8**, 304.
55. Ginalski, K., Elofsson, A., Fischer, D. & Rychlewski, L. (2003). 3D-Jury: a simple approach to improve protein structure predictions. *Bioinformatics*, **19**, 1015–1018.
56. Cooper, D. R., Boczek, T., Grelewska, K., Pinkowska, M., Sikorska, M., Zawadzki, M. & Derewenda, Z. (2007). Protein crystallization by surface entropy reduction: optimization of the SER strategy. *Acta Crystallogr. Sect. D*, **63**, 636–645.
57. Goldschmidt, L., Cooper, D. R., Derewenda, Z. S. & Eisenberg, D. (2007). Toward rational protein crystallization: a Web server for the design of crystallizable protein variants. *Protein Sci.* **16**, 1569–1576.

58. Derewenda, Z. S. & Vekilov, P. G. (2006). Entropy and surface engineering in protein crystallization. *Acta Crystallogr. Sect. D*, **62**, 116–124.
59. Derewenda, Z. S. (2004). Rational protein crystallization by mutational surface engineering. *Structure*, **12**, 529–535.
60. Weaver, A. J., Sullivan, W. P., Felts, S. J., Owen, B. A. & Toft, D. O. (2000). Crystal structure and activity of human p23, a heat shock protein 90 co-chaperone. *J. Biol. Chem.* **275**, 23045–23052.
61. Bagneris, C., Bateman, O. A., Naylor, C. E., Cronin, N., Boelens, W. C., Keep, N. H. & Slingsby, C. (2009). Crystal structures of alpha-crystallin domain dimers of alphaB-crystallin and Hsp20. *J. Mol. Biol.* **392**, 1242–1252.
62. Holm, L., Kaariainen, S., Rosenstrom, P. & Schenkel, A. (2008). Searching protein structure databases with DaliLite v.3. *Bioinformatics*, **24**, 2780–2781.
63. Holm, L., Kaariainen, S., Wilton, C. & Plewczynski, D. (2006). Using Dali for structural comparison of proteins. *Curr. Protoc. Bioinf.* Chapter 5, Unit 5.5.
64. Zhang, M., Kadota, Y., Prodromou, C., Shirasu, K. & Pearl, L. H. (2010). Structural basis for assembly of Hsp90–Sgt1–CHORD protein complexes: implications for chaperoning of NLR innate immunity receptors. *Mol. Cell*, **39**, 269–281.
65. Kadota, Y., Shirasu, K. & Guerois, R. (2010). NLR sensors meet at the SGT1–HSP90 crossroad. *Trends Biochem. Sci.* **35**, 199–207.
66. Ali, M. M., Roe, S. M., Vaughan, C. K., Meyer, P., Panaretou, B., Piper, P. W. *et al.* (2006). Crystal structure of an Hsp90–nucleotide–p23/Sba1 closed chaperone complex. *Nature*, **440**, 1013–1017.
67. Singh, M., Gonzales, F. A., Cascio, D., Heckmann, N., Chanfreau, G. & Feigon, J. (2009). Structure and functional studies of the CS domain of the essential H/ACA ribonucleoparticle assembly protein SHQ1. *J. Biol. Chem.* **284**, 1906–1916.
68. Finn, R. D., Tate, J., Mistry, J., Coggill, P. C., Sammut, S. J., Hotz, H. R. *et al.* (2008). The Pfam protein families database. *Nucleic Acids Res.* **36**, D281–D288.
69. Bateman, A., Birney, E., Cerruti, L., Durbin, R., Etwiller, L., Eddy, S. R. *et al.* (2002). The Pfam protein families database. *Nucleic Acids Res.* **30**, 276–280.
70. Bhattacharya, S., Lee, Y. T., Michowski, W., Jastrzebska, B., Filipek, A., Kuznicki, J. & Chazin, W. J. (2005). The modular structure of SIP facilitates its role in stabilizing multiprotein assemblies. *Biochemistry*, **44**, 9462–9471.
71. Santelli, E., Leone, M., Li, C., Fukushima, T., Preece, N. E., Olson, A. J. *et al.* (2005). Structural analysis of Siah1–Siah-interacting protein interactions and insights into the assembly of an E3 ligase multiprotein complex. *J. Biol. Chem.* **280**, 34278–34287.
72. Clark, J. I. & Muchowski, P. J. (2000). Small heat-shock proteins and their potential role in human disease. *Curr. Opin. Struct. Biol.* **10**, 52–59.
73. Lupas, A. (1997). Predicting coiled-coil regions in proteins. *Curr. Opin. Struct. Biol.* **7**, 388–393.
74. Zhu, H., Domingues, F. S., Sommer, I. & Lengauer, T. (2006). NOXclass: prediction of protein–protein interaction types. *BMC Bioinf.* **7**, 27.
75. Perez, D. E., Hoyer, J. S., Johnson, A. I., Moody, Z. R., Lopez, J. & Kaplinsky, N. J. (2009). BOBBER1 is a noncanonical *Arabidopsis* small heat shock protein required for both development and thermotolerance. *Plant Physiol.* **151**, 241–252.
76. Burdette, A. J., Churchill, P. F., Caldwell, G. A. & Caldwell, K. A. (2010). The early-onset torsion dystonia-associated protein, torsinA, displays molecular chaperone activity *in vitro*. *Cell Stress Chaperones*, **15**, 605–617.
77. Cherepkova, O. A., Lyutova, E. M., Eronina, T. B. & Gurvits, B. Y. (2006). Chaperone-like activity of macrophage migration inhibitory factor. *Int. J. Biochem. Cell Biol.* **38**, 43–55.
78. Saibil, H. R. (2008). Chaperone machines in action. *Curr. Opin. Struct. Biol.* **18**, 35–42.
79. McHaourab, H. S., Godar, J. A. & Stewart, P. L. (2009). Structure and mechanism of protein stability sensors: chaperone activity of small heat shock proteins. *Biochemistry*, **48**, 3828–3837.
80. Horwitz, J. (1992). Alpha-crystallin can function as a molecular chaperone. *Proc. Natl Acad. Sci. USA*, **89**, 10449–10453.
81. Jakob, U., Gaestel, M., Engel, K. & Buchner, J. (1993). Small heat shock proteins are molecular chaperones. *J. Biol. Chem.* **268**, 1517–1520.
82. Lee, G. J., Roseman, A. M., Saibil, H. R. & Vierling, E. (1997). A small heat shock protein stably binds heat-denatured model substrates and can maintain a substrate in a folding-competent state. *EMBO J.* **16**, 659–671.
83. Jakob, U., Lilie, H., Meyer, I. & Buchner, J. (1995). Transient interaction of Hsp90 with early unfolding intermediates of citrate synthase. Implications for heat shock *in vivo*. *J. Biol. Chem.* **270**, 7288–7294.
84. Holaska, J. M., Black, B. E., Love, D. C., Hanover, J. A., Leszyk, J. & Paschal, B. M. (2001). Calreticulin is a receptor for nuclear export. *J. Cell Biol.* **152**, 127–140.
85. Guo, L., Groenendyk, J., Papp, S., Dabrowska, M., Knoblach, B., Kay, C. *et al.* (2003). Identification of an N-domain histidine essential for chaperone function in calreticulin. *J. Biol. Chem.* **278**, 50645–50653.
86. Galigniana, M. D., Harrell, J. M., O'Hagen, H. M., Ljungman, M. & Pratt, W. B. (2004). Hsp90-binding immunophilins link p53 to dynein during p53 transport to the nucleus. *J. Biol. Chem.* **279**, 22483–22489.
87. Nery, F. C., Zeng, J., Niland, B. P., Hewett, J., Farley, J., Irimia, D. *et al.* (2008). TorsinA binds the KASH domain of nesprins and participates in linkage between nuclear envelope and cytoskeleton. *J. Cell Sci.* **121**, 3476–3486.
88. Longenecker, K., Read, P., Derewenda, U., Dauter, Z., Liu, X., Garrard, S. *et al.* (1999). How RhoGDI binds Rho. *Acta Crystallogr. Sect. D*, **55**, 1503–1515.
89. Hoffman, G. R., Nassar, N. & Cerione, R. A. (2000). Structure of the Rho family GTP-binding protein Cdc42 in complex with the multifunctional regulator RhoGDI. *Cell*, **100**, 345–356.
90. Sheffield, P., Garrard, S. & Derewenda, Z. (1999). Overcoming expression and purification problems of RhoGDI using a family of "Parallel" expression vectors. *Protein Expression Purif.* **15**, 34–39.
91. Schneider, T. R. & Sheldrick, G. M. (2002). Substructure solution with SHELXD. *Acta Crystallogr. Sect. D*, **58**, 1772–1779.
92. Sheldrick, G. M. (2002). Macromolecular phasing with SHELXE. *Z. Kristallogr.* **217**, 644–650.

93. Morris, R. J., Perrakis, A. & Lamzin, V. S. (2003). ARP/wARP and automatic interpretation of protein electron density maps. *Methods Enzymol.* **374**, 229–244.
94. Murshudov, G. N., Vagin, A. A. & Dodson, E. J. (1997). Refinement of macromolecular structures by the maximum-likelihood method. *Acta Crystallogr. Sect. D*, **53**, 240–255.
95. Adams, P. D., Afonine, P. V., Bunkoczi, G., Chen, V. B., Davis, I. W., Echols, N. *et al.* (2010). PHENIX: a comprehensive Python-based system for macromolecular structure solution. *Acta Crystallogr. Sect. D*, **66**, 213–221.
96. Jones, T. A., Zou, J. Y., Cowan, S. W. & Kjeldgaard, M. (1991). Improved methods for binding protein models in electron density maps and the location of errors in these models. *Acta Crystallogr. Sect. A*, **47**, 110–119.
97. Emsley, P. & Cowtan, K. (2004). Coot: model-building tools for molecular graphics. *Acta Crystallogr. Sect. D*, **60**, 2126–2132.
98. Davis, I. W., Leaver-Fay, A., Chen, V. B., Block, J. N., Kapral, G. J., Wang, X. *et al.* (2007). MolProbity: all-atom contacts and structure validation for proteins and nucleic acids. *Nucleic Acids Res.* **35**, W375–W383.
99. Laskowski, R. A., McArthur, M. W., Moss, D. S. & Thornton, J. M. (1993). PROCHECK: a program to check the stereochemical quality of protein structures. *J. Appl. Crystallogr.* **26**, 282–291.
100. Ashkenazy, H., Erez, E., Martz, E., Pupko, T. & Ben-Tal, N. (2010). ConSurf 2010: calculating evolutionary conservation in sequence and structure of proteins and nucleic acids. *Nucleic Acids Res.* **38**, W529–W533.
101. Landau, M., Mayrose, I., Rosenberg, Y., Glaser, F., Martz, E., Pupko, T. & Ben-Tal, N. (2005). ConSurf 2005: the projection of evolutionary conservation scores of residues on protein structures. *Nucleic Acids Res.* **33**, W299–W302.